

Review

# Recent Trends in Biosensors for Quinolone Detection: A Comprehensive Review

Fabian Thurner  and Fatima AlZahra'a Alatraktchi \* 

Department of Science and Environment, Roskilde University, 4000 Roskilde, Denmark; fabianth@ruc.dk

\* Correspondence: alzahraa@ruc.dk

**Abstract:** Quinolones represent a vast family of antibiotics used extensively around the globe in human and veterinary medicine. Over the past decade, the field of biosensors for quinolone detection has experienced significant growth, thanks to the advancements in nanotechnology. These biosensors have emerged as a promising tool for fast and accurate point-of-care detection of quinolones. Although research efforts have proven that it is possible to detect quinolones in complex matrices and in relevant concentration ranges, the complexity of the sensor functionalization and the risk of limited reproducibility has hindered the transfer to real-life applications. This review holistically summarizes existing electrochemical quinolone sensors in comparison to optical and piezoelectric sensors and discusses the challenges that remain to be solved.

**Keywords:** quinolones; biosensors; antibiotics; detection; electrochemical sensors; optical sensors

## 1. Introduction

Despite the countless benefits of antibiotics, their widespread use has led to the emergence of antibiotic resistant bacteria [1]. To help mitigate the upsurge of resistant microorganisms, accurate and robust testing for antibiotics in the healthcare and environmental sectors is of utmost importance. The main analytical methods to determine antibiotic concentrations are HPLC and HPLC-MS, while rapid methods comprise ELISA and microfluidic chips [2–5]. However, in recent years, biosensors have surfaced as a promising tool for the rapid and reliable point-of-care detection of antibiotics in clinical, food safety, and environmental settings [6–9].

Within the domain of antibiotics, a vast class known as quinolones holds particular significance. Quinolones are considered core therapies to treat both community-acquired and hospital-acquired infections in the last six decades [10,11]. Members of the quinolone group share a bicyclic core structure related to the substance 4-quinolone [11]. Their increasing popularity can primarily be attributed to their moderate to excellent bioavailability and pharmacokinetic properties, which allow them to provide treatment of a variety of Gram-negative and Gram-positive bacterial infections [11,12]. Constant reiteration of quinolones over the years has led to improvements in their pharmacological activity, pharmacokinetics, and pharmacodynamics, making a world devoid of the drug hard to imagine [11].

Multiple reviews are available that discuss different aspects of sensors used for the detection of quinolones. In a holistic review, Wang et al. summarized electrochemical sensors developed to detect a broad range of antibiotics including quinolones. They compared various nanomaterials used in sensor architecture as well as explained existing sample pretreatments [13]. Two reviews have been published on specific types of biosensors, immunosensors and aptasensors, and their role in quinolone detection: Pollap et al. summarized electrochemical immunosensors and Mehlhorn and colleagues provided insights into aptamer-based biosensors [14,15].

Literature focusing solely on quinolone detection has also been published: through a focused lens, Jiwanti et al. explored carbon-based electrodes used in electrochemical



**Citation:** Thurner, F.; Alatraktchi, F.A. Recent Trends in Biosensors for Quinolone Detection: A Comprehensive Review. *Chemosensors* **2023**, *11*, 493. <https://doi.org/10.3390/chemosensors11090493>

Academic Editor: Edward P. C. Lai

Received: 15 July 2023

Revised: 30 August 2023

Accepted: 3 September 2023

Published: 6 September 2023



**Copyright:** © 2023 by the authors. Licensee MDPI, Basel, Switzerland. This article is an open access article distributed under the terms and conditions of the Creative Commons Attribution (CC BY) license (<https://creativecommons.org/licenses/by/4.0/>).

sensors to detect quinolone antibiotics. They discuss the utilization of modified and unmodified carbon-based electrodes, by which they also categorize biosensors and non-biosensors [16]. In a review from 2019, Majdinasab et al. covered optical and electrochemical sensors and biosensors for the detection of quinolones. They provide the reader with a compelling overview over various types of sensors, sharing valuable insights into the many types of sensors that exist [17]. Finally, Ansari et al. published a focused review on the optical and electrochemical biosensing approaches specifically for ciprofloxacin in food and environment samples [18].

Expanding and complementing existing work, this review aims to provide a novel overview of recent advances in the field of biosensors for the detection of quinolone antibiotics. It will review biosensors that have been developed up to the present day, with particular emphasis on innovative approaches developed since 2019. The biosensors will be categorized into immunosensors, aptasensors, and enzyme-based sensors and reviewed based on their operating principle and the quinolone drug they can detect. Moreover, they will be compared to each other in terms of their limit of detection (LoD), linear range, biorecognition element, transducer platform, operating medium, and response time. Finally, the sensor lifetime and matrix interferences will be discussed.

### 1.1. Antibiotic Pollution of the Environment—A Regulatory Perspective

Despite their countless benefits, antibiotics have polluted the environment [19]. Mainly used in animal husbandry and human medicine, they enter the ecosystem through excreta and the improper disposal of medicinal products [20]. Once in the environment, antibiotics facilitate the development of antibiotic-resistant microbes and pose serious risks to human health [20].

Presently, regulations on the surveillance and quantification of antibiotics in the environment, the establishment of safe levels, and the examination of their environmental impact are lacking on a global level [20].

Thankfully, in the food industry, more stringent regulations on antibiotics have been set by the World Health Organization (WHO) and the Food and Agriculture Organization of the United Nations (FAO), which established the Codex Alimentarius, a collection of global standards and guidelines ensuring worldwide food safety.

During livestock breeding, food-producing animals such as cattle poultry or swine are typically treated with quinolones, resulting in the accumulation of antibiotic residues in edible tissues such as eggs, meat, and dairy products. To ensure food safety, regulatory agencies have established maximum residue limits (MRLs), representing the maximum legally allowed amount of a given antibiotic in a particular food. As different countries have set different MRLs for different foods from different animals, each of which varies in terms of the specific quinolone, it is not possible to provide an exhaustive overview of this issue in this review. However, as the most prominent medium in which quinolone biosensors have been tested is milk, Table 1 presents an overview of MRLs set by the Codex Alimentarius. The antibiotics mentioned are based on the OIE list of antimicrobial agents of veterinary importance (2018) and the data were taken from the online service “antibioticsfinder” [21,22].

**Table 1.** MRLs of selected quinolones set by the Codex Alimentarius in bovine milk.

Antibiotic	MRL (ppb)	MRL (mol)
Ciprofloxacin	100	302 nM
Danofloxacin	30	84 nM
Difloxacin	Not allowed	Not allowed
Enrofloxacin	100	278 nM
Flumequin	50	191 nM
Marbofloxacin	75	207 nM

**Abbreviations:** MRLs, maximum residue limits; ppb, parts per billion.

### 1.2. A Brief History of Quinolones

The history of quinolones is marked by countless iterations, innovations, and expansions throughout the years—a fact reflected by the multitude of potent members of the drug commercially available today.

In 1967, nalidixic acid was approved for clinical use to treat uncomplicated urinary tract infections (UTIs), but it was found shortly after that various species rapidly developed resistance toward it (Figure 1A) [23]. Because of adverse effects like low serum concentrations and high minimum inhibitory concentrations, nalidixic acid fell into neglect until the advent of fluoroquinolones in the 1970s and 1980s [11,24]. Chemically adjusting quinolones to turn them into fluoroquinolones broadened their spectrum of antimicrobial coverage as well as enhanced their pharmacokinetics [11,24]. Some of the “second generation” antibiotics patented during this time are still in use today including ofloxacin, ciprofloxacin, and norfloxacin (Figure 1B) [23,24].

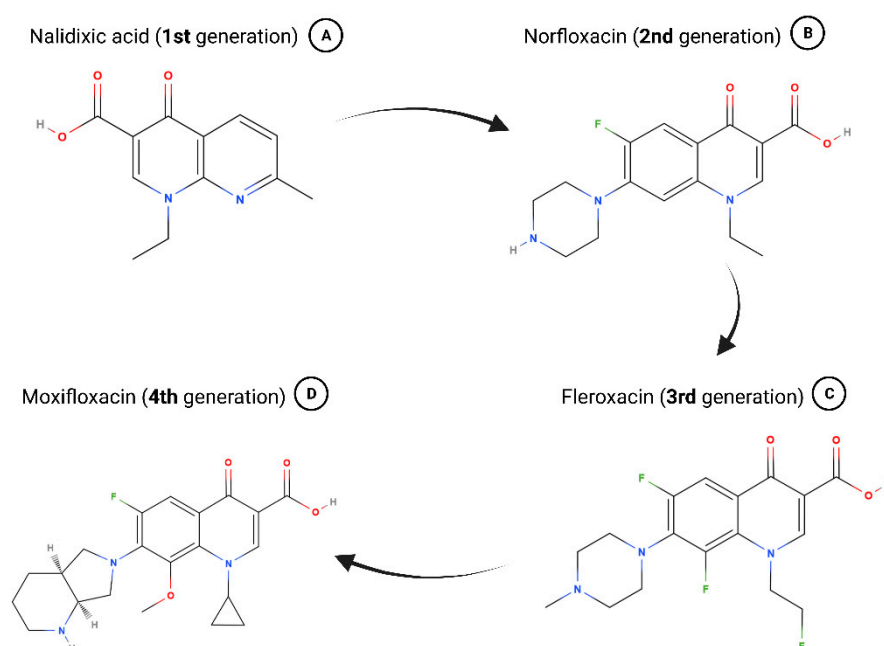


**Figure 1.** Chemical formulas of selected 1st-, 2nd-, 3rd-, and 4th-generation quinolones. (A) Nalidixic acid was approved in 1967 and represents the beginning of the history of quinolones. (B) Addition of a fluor atom marks fluoroquinolones and many are still used today (e.g., norfloxacin). (C) Due to several changes in chemical structure, fleroxacin marks the beginning of 3rd-generation quinolones. (D) The most recent 4th-generation quinolones have strong antimicrobial activity and greatly improved anaerobic coverage (e.g., moxifloxacin). Chemical structures retrieved from the PubChem database via MolView. Created with [bioRender.com](https://www.bioRender.com).

Fleroxacin marks the beginning of the “third generation” of quinolones, which exhibited greatly broadened anti-microbial activity due to several changes in its chemical structure (Figure 1C) [11,24]. Hallmarks for the “fourth generation” of quinolones, the most recent one, are strong antimicrobial activity including against atypical pathogens and improved anaerobic coverage (Figure 1D) [11,25,26].

### 1.3. How Quinolones Hijack the Enzymatic Machinery of Prokaryotes

Most bacterial species encode DNA gyrase and topoisomerase IV, both members of the type II topoisomerases. These well-studied enzymes can introduce transient double strand breaks in DNA, passing through a segment of DNA and religating the ends. By that, they regulate the supercoiling (over- or underwinding) of DNA [27–29].

Type II topoisomerases are essential in shaping the DNA topology of prokaryotes, making them an indispensable part of their enzymatic repertoire by aiding recombination

events and releasing torsion stress during replication via the introduction of transient DNA breaks [27,28,30–33]. This makes them an attractive target for quinolones, who exploit the fact that the accumulation of topoisomerase DNA cleavage complexes is linked to significant bactericidal activity [26,33–35]. Quinolones act by increasing the cellular concentration of topoisomerase cleavage complexes, which leads to the conversion of transient to permanent DNA double-strand breaks throughout the microbial genome. Consequently, the SOS response is triggered, and cells undergo apoptosis [26,33,36]. In our favor, quinolones act specifically on bacterial DNA, sparing the human genome from this fate when ingesting the antibiotic [26].

#### 1.4. How Prokaryotes Fight Back by Developing Resistance

Following the profound groundwork done by Flemming and Ehrlich, the period from 1950 to 1970 has been deemed a golden era in the discovery of novel classes of antibiotics [37]. Although the positive effects that antibiotics have on our society are anything but negligible, their misuse can be strongly felt due to the global emergence of antibiotic resistant bacteria. This has become a significant public health concern as the radiation of multi-resistant bacteria has led to an increase in treatment failures, prolonged hospital stays, and higher mortality rates [37].

A comprehensive study from 2022 estimated that 4.95 million deaths have been associated with bacterial antimicrobial resistance in 2019. The top six pathogens (*Escherichia coli*, followed by *Staphylococcus aureus*, *Klebsiella pneumoniae*, *Streptococcus pneumoniae*, *Acinetobacter baumannii*, and *Pseudomonas aeruginosa*) accounted for 3.57 million deaths associated with bacterial antimicrobial resistance [38].

In a recent study, Deku and colleagues investigated the burden of bacteria specifically resistant to four fluoroquinolones at the Ho Teaching Hospital in Ghana. They found that 90 out of 135 *Escherichia coli* isolates were resistant to at least one of the four fluoroquinolone drugs investigated [39].

To adapt to the rise in the misuse of quinolone antibiotics worldwide, bacteria developed a variety of molecular mechanisms underlying quinolone resistance. One way involves mutations in the *quinolone resistance determining region* (QRDR) of two essential target enzymes of quinolones—DNA gyrase and topoisomerase IV [40,41]. Although they are less commonly found, mutations in domains outside of QRDR have also been shown to play a causative role in the emergence of resistance [40,42,43].

Moreover, mutations that reduce the levels of drug concentration in the cell are favored. This can mainly be achieved in two ways: actively pumping the drug out of the cell via efflux mechanisms, or reducing the uptake of the drug such as by the downregulation of porin channels [40,44–46]. In *Staphylococcus aureus*, expression of the efflux pump *norA* results in 4-fold to 32-fold increase in the minimum inhibitory concentration (MIC) to numerous substrates [47].

#### 1.5. Detection of Quinolones—From Classical Methods to Biosensors

To detect and quantify trace amounts of antibiotics, either high-performance liquid chromatography (HPLC) alone or coupled with an elaborate detection system (HPLC-MS) is considered the gold standard to detect and quantify antibiotics in a variety of samples [2,48]. Such systems come with high sensitivity and the capability to analyze complex multi-quinolone samples [49–54]. Cavazos-Rocha et al. developed a method using HPLC for the simultaneous quantification of multiple fluoroquinolones and oxazolidinone antibiotics in a mixed sample [54]. Via HPLC-MS, Wei et al. demonstrated the simultaneous detection of nine quinolone antibiotics with excellent detection limits between 1 and 100 ng/mL [50]. Using liquid chromatography in tandem with MS (LC-MS), Chang et al. could detect 18 quinolone residues simultaneously in milk, chicken, pork, and shrimp [53]. Annunziata et al. reported on the development and validation of an LC-MS method capable of detecting 11 quinolones in muscle and eggs, demonstrating great recovery values in both matrices [52]. Optimizing separation and detection conditions, Lombardo-Agüi

et al. determined 19 quinolones in water samples using ultra high-performance liquid chromatography (UHPLC) with MS in 4 min [49]. Chromatographic methods to detect quinolones offer great sensitivity, reproducibility, and are great for validation and multidrug analysis. However, they are high in cost, non-portable, and require elaborate sample preparation that differs across different biological, food, and environmental samples [55].

To rapidly detect quinolones, microfluidic chip systems and the enzyme-linked immunosorbent assay (ELISA) have become a widely used technique.

Microfluidic analysis scores with its low-cost, portable, and rapid detection of antibiotic residues [5]. One of their advantages is that they can easily be integrated with various detection methods such as fluorescence, chemiluminescence, electrochemistry, or even mass spectrometry [5,56–59].

ELISA is based on the reaction of antigens and antibodies, which give the assay its high specificity and selectivity [3,4]. In an excellent review by Pan et al., recent advances in immunoassays for quinolone detection are reported [60]. A prime example of this is an ELISA-based method developed by Wen and colleagues. They were able to manufacture a generic antibody capable of recognizing nearly all fluoroquinolones with high specificity and selectivity [61]. As another example, Huet and colleagues developed a direct competitive ELISA capable of detecting a broad range of 15 quinolones [62]. Yadoung and colleagues incorporated the IgY antibody purified from egg yolk in their indirect competitive ELISA. They could detect low levels of ciprofloxacin, norfloxacin, and enrofloxacin with good recovery values. Their study confirmed that IgY could be a promising choice for the detection of antibiotic residues [63]. Finally, in a recent study from 2023, an ELISA was developed based on a broad-spectrum antibody to determine 13 fluoroquinolones in the edible frog *Rana catesbeianus* [64].

However, ELISA also comes with limitations such as a high possibility of false positives/negatives, antibody instability, and refrigerated transport and storage [65]. Furthermore, in an era of automation and high throughput, ELISA may not meet these demands [4].

The discovery of biosensors dates to 1956, when Leland C. Clark Jr. developed a device to detect oxygen in blood [66]. Today, biosensors are an integral part of our lives in areas as diverse as environmental and food quality monitoring, healthcare, and industrial manufacturing, and it is hard to envision a world without them [67]. Due to their ease of use and possibility for on-site-detection and point-of-care application, it should come as no surprise that they are indispensable in the rapid and reliable detection of antibiotics including the family of quinolones.

## 2. Biosensors

According to IUPAC, a biosensor is “a device that uses specific biochemical reactions mediated by isolated enzymes, immunosystems, tissues, organelles or whole cells to detect chemical compounds usually by electrical, thermal or optical signals [68]”.

Broadly speaking, a biosensor consists of two essential elements: the biorecognition element and the transducer. The biorecognition element is the biological specificity-conferring mechanism of the sensor (Figure 2). It has affinity for a target analyte and mediates contact between it and the rest of the sensor [69–71]. It is the biological nature of the recognition element that gives the sensor the name of a biosensor.

The transducer element is what converts the biorecognition event into a quantifiable signal that provides valuable information about the concentration of the analyte of interest [69–71]. The signal output of transducers can be of various types, but most are operating on either optical or electrical signals [70,71].

There are many ways to classify biosensors: they can be grouped either by their biorecognition element, or by the type of transducer or by a combination of both [69]. In this review, we chose to classify them according to their biorecognition element by grouping them into the three distinct, most prominent groups in the field of quinolone detection: immunosensors, aptasensors, and enzymatic sensors.

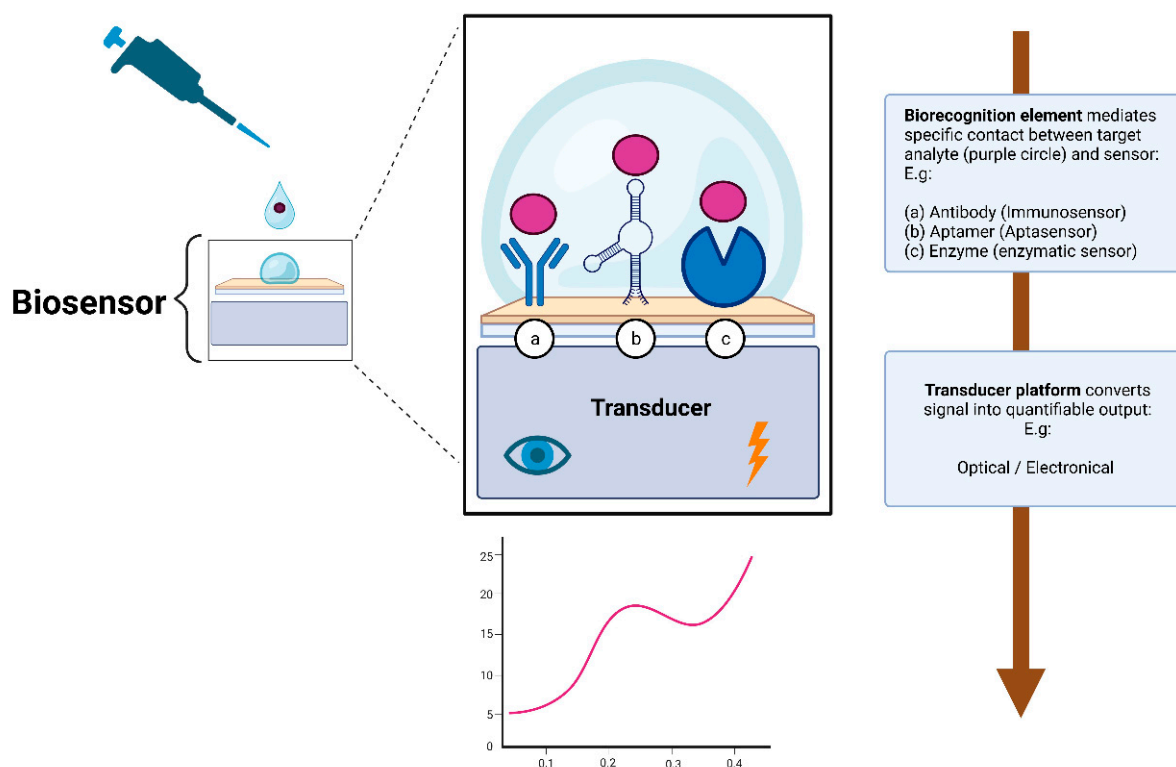


**Figure 2.** Simplified illustration depicting the working principle of a biosensor. The biorecognition element (hence the name biosensor) mediates specific and sensitive contact with the rest of the sensor. To stay within the scope of this review, only the three most prominent biorecognition elements are depicted: (a) immunosensors, (b) aptasensors, or (c) enzymatic sensors. The transducer then converts the signal into quantifiable data, providing invaluable insights about the concentration of the target analyte. Created with [bioRender.com](https://www.biorender.com).

The electrochemical and optical transducers are the most widely used transducers in quinolone biosensor architectures. Due to their complex fundamental principles, it is beyond the scope of this review to examine them in detail. The reader is referred to the following reviews on optical and electrochemical biosensors, which cover broad aspects and provide an exhaustive overview of the subject [72–75]. Furthermore, the explanation of different electrochemical techniques lies outside of the scope of this review. Extensive literature already exists on the working principles behind the cyclic voltammetry (CV), differential pulse voltammetry (DPV) and electrochemical impedance spectroscopy (EIS) methods [75–79].

### 2.1. Immunosensors Used for Quinolone Detection

Immunosensors are biosensors that use antibodies as their recognition element. They have gained considerable acceptance due to their unparalleled affinity for target analytes, making them an indispensable part of quinolone biosensors today. Table 2 summarizes immunosensors used for quinolone detection and compares them in terms of the target, detection strategy, transducer, limit of detection (LOD), linear range, response time, and sample type.

In 2022, Liu and colleagues came up with a novel optical immunosensor for quinolone detection inspired by allosteric transcription factors (aTFs) and strand displacement amplification (SDA). aTFs undergo conformation changes upon binding to a ligand, which alters their affinity to DNA motifs. Due to their innate architecture, they can act as a switch to turn genes on and off and are therefore widely used in fields such as synthetic biology [80–82]. Isothermal amplification strategies such as SDA have been gaining attention in recent years as the new “gold standard” for nucleic acid amplification. As the name

implies, they require only a constant working temperature as opposed to PCR, which needs various temperature ranges. This comes with many benefits such as the possibility for high throughput analysis, single workflows and the mimicking of *in vivo* mechanisms [83]. Liu and colleagues used SDA with aTFs and developed a novel biosensor based on the antibody controlled isothermal strand displacement amplification (ACISDA) system [81,84,85]. They explored a novel approach based on antigen-labelled DNA as the primer for SDA combined with a competitive reaction: without antigen in the sample, the antibodies would bind to the labelled primer, preventing the SDA reaction from happening. In the presence of antigen in the sample, the antibodies will dissociate from the modified primer, which in turn triggers the SDA reaction to start. The SDA reaction produces nucleotide sequences that spontaneously change conformation and fold into G-quadruplex structures that bind with the dye Thioflavin T (ThT) to augment the output fluorescent signal [81,86–88]. Using this creative system, in 90 min, Liu and colleagues were able to detect the quinolone norfloxacin in a linear range of 0.1–500 ng/mL with a detection limit of 0.04 ng/mL. The system demonstrated good stability after it was pre-distributed and freeze-dried at 4 °C for one month, and would therefore facilitate the detection of norfloxacin in field testing [81].

Another brilliant example of an optical antibody-based biosensor developed recently to detect trace amounts of norfloxacin comes with a twist: it is reusable and smartphone-facilitated [89]. Cheng et al. argued that although most optical sensor designs are excellent solutions for various problems, their intricate architecture limits their scalability and portability [89]. In their study, they worked around this problem by integrating a smartphone into a portable optical system paired with microfluidics. To miniaturize the sensor, they used an asymmetric Y-shaped fiber optic coupler (Y-FOC) that could simultaneously transmit excitation light and collect fluorescence [89]. In an elaborate process, they functionalized a bio-probe by coating it with norfloxacin antigen solution. After labelling norfloxacin antibodies to Cyanine 5.5 NHS ester (Cy5.5) and mixing it together with norfloxacin containing sample solutions, they introduced the sample into the previously functionalized bio-probe. In an indirect competitive immunoreactive manner, the Cy5.5 labelled antibodies bind the coating-antigen immobilized onto the fiber biosensor surface and transmit excited light. The intensity of fluorescence measured by Y-FOC is therefore inversely proportional to the norfloxacin sample concentration. Using this creative approach, Chen and colleagues were able to detect norfloxacin at concentrations as low as 0.15 ng/mL with broad linear ranges from 5.6 to 256.8 ng/mL while keeping a rapid response time of merely 10 min. Finally, they showed that the fiber bio-probe had an excellent lifetime, losing only 10% of its response after 4 weeks stored at room temperature [89]. They digitalized their system by creating an auxiliary smartphone application allowing for fast and quantitative on-site detection, laying important groundwork for the future of portable biosensor designs [89].

Pushed by the advent of nanotechnology, recent progress has also been made in the field of electrochemical immunosensors for quinolone detection. In 2021, Chaudhary et al. incorporated lanthanum oxide nanoparticles ( $n\text{La}_2\text{O}_3$  NPs) in their design for a novel immunosensor to detect trace amounts of ciprofloxacin [90].

Due to interesting properties such as the low environmental impact, the high stability, and the high dielectric constant of rare earth metals, they have found their way into various applications such as the development of biosensors [91–93]. Lanthanum oxide, one of the rare earth metals, was used by Chaudhary and colleagues to synthesize nanoparticles ( $n\text{La}_2\text{O}_3$  NPs). To build a stable immobilization matrix for ciprofloxacin antibodies, they functionalized indium tin oxide (ITO) coated glass electrodes with the nanoparticles. Using differential pulse voltammetry, they achieved excellent biosensing parameters with broad linear ranges of 0.001–0.5 ng/mL and 1–1000 ng/mL and a LOD of 0.001 ng/mL [90]. Furthermore, their approach ranks among the quickest in quinolone detection, requiring just 12 min for a response. Stability tests suggest that the immunosensor has a good shelf life of up to 20 days [90].

Continuing with electrochemical immunosensors based on rare earth metals, Yadav et al. recently presented a label-free amperometric biosensor for the antibiotic norfloxacin

based on a chitosan-yttria nanocomposite [94]. For the first time, they successfully synthesized the rare earth metal oxide  $nY_2O_3$  and integrated it into the development of a novel electrochemical platform for the detection of norfloxacin. To build a stable composite, they covered the glassy carbon substrate with indium tin oxide (ITO) and functionalized the electrode with anti-ciprofloxacin antibodies in an elaborate protocol discussed in their publication in greater depth. They could confirm successes of the iterative functionalization process by DPV measurements and analyzed the sensor on various fronts such as structural characterizations and electrochemical studies. In the end, they successfully developed a sensor that could detect norfloxacin down to 1.236 pg/mL within only 10 min of incubation time. Moreover, the sensor was successfully used to detect the antibiotic in spiked urine samples [94].

Piezoelectric immunosensors have recently surfaced as a promising tool to detect small amounts of analytes with high accuracy. Gravimetric piezoelectric sensors act as a “scale” as changes in their mass go hand in hand with changes in the frequency, amplitude, and phase of the transducer [95]. These properties can be used to directly detect an immunoreaction by mass alone [96]. Due to the unique properties of carbon nanotubes (CNTs) like high electrical conductivity, chemical stability, and unparalleled mechanical strength-to-weight ratio, they have achieved high praise in the development of biosensors [97–99].

Bizina and colleagues managed to merge carbon nanotubes with magnetic nanoparticles ( $Fe_3O_4$ NPs) to form two kinds of magnetic carbon composites (MCNC1/2) [100]. Introducing piezoelectricity into this concept, the composite was then used as the recognition layer for a novel piezoelectric immunosensor. The result of this creative approach was the sensitive and selective determination of ciprofloxacin in various food products with a LOD of 2 ng/mL for MCNC1 and 8 ng/mL for MCNC2 [100]. Furthermore, Bizina and colleagues reported that the linear range of the developed sensor was reported to be 5–400 ng/mL [100].

**Table 2.** Immunosensors for quinolone detection.

Transducer	Target	Working Principle	LOD	Linear Range	Response Time	Medium	Reference
Optical	NOR	Antibody conjugated with $NaYF_4:Yb,Er$ UCNPs, and antigen-modified polystyrene particles	10 pg/mL	10 pg/mL–10 ng/mL	/	Milk, honey, tissue samples of animals	[101]
Optical	NOR	Simultaneous detection of several antibiotics with SERS-based multiple immuno-nanoprobe via ICA	0.55 pg/mL	0.1 pg/mL–1.0 ng/mL	/	Milk	[102]
Optical	NOR	Reusable smartphone-facilitated mobile fluorescence sensor/asymmetric Y-shaped fiber optic coupler for simultaneous transmission of light and collected fluorescence	0.15 ng/mL	5.6–256.8 ng/mL	15 min	Water	[89]
Optical	NOR	Evanescence wave fiber optics	1.89 ng/mL	/	/	Water	[103]
Optical	NOR	Antibody controlled isothermal chain displacement amplification	0.04 ng/mL	0.1–500 ng/mL	90 min	Artificial urine, milk, chicken, water	[81]
Optical	ENR	Near-infrared fluorescence-based multiplex ICA	0.08 ng/mL	0.08–2.0 ng/mL	10 min	Milk	[104]

Table 2. Cont.

Transducer	Target	Working Principle	LOD	Linear Range	Response Time	Medium	Reference
Optical	ENR	MICA/QICA	1.0 ng/mL (buffer), 5.0 µg/kg (animal tissue), 10.0 ng/mL (milk)	/	20 min	Buffer, animal tissue, milk	[105]
Optical	OFL	ICA based on binding of OFL to colloidal gold-labeled antibodies	30 ng/mL	/	10 min	Milk	[106]
Optical	OFL	ICA for simultaneous detection of several compounds, based on multicolor QDs	0.3 ng/mL	1.5–200 ng/mL	10 min	Milk	[107]
Optical	CIPR	CIP-protein conjugate labeled with near infrared dye/fluorescent polarization emission signal	1 ng/mL	/	/	Milk	[108]
Optical	ENR, CIPR, NOR	FRET between FQs and labeled AuNPs for FQs Mab connected $\beta$ -NaLuF <sub>4</sub> :Yb,Er,G	0.19–0.32 ng/mL	1–80 ng/mL	/	Water samples	[109]
Electrochemical (EIS)	CIPR	SPCE/EDC/NHS/IgG electrode	0.025 ng/mL	0.01 ng/mL–1.0 µg/mL	22 min	Wastewater	[110]
Electrochemical (EIS)	CIPR	Polypyrrole-antibiotic model film/label-free	0.994 pg/mL	/	/	Aqueous solution	[111]
Electrochemical (EIS)	CIPR	Electropolymerization of pyrrole-NHS/antibody grafting	10 pg/mL	/	/	Aqueous solution	[112]
Electrochemical (amperometry)	CIPR	Haptenized enzyme/magnetic graphite-epoxy composite	0.009 ng/mL	0.043–7.38 ng/mL	/	Spiked milk	[113]
Electrochemical (DPV)	CIPR	BSA/anti-CIPR/APTES/nLa <sub>2</sub> O <sub>3</sub> /ITO	0.001 ng/mL	0.001–0.5 ng/mL 1–1000 ng/mL	12 min	Milk	[90]
Electrochemical (CV, ACIP)	CIPR	Electrodeposited polyaniline used to immobilize biotinylated CIPR-Antibody	/	0.1–100 ng/mL	30 min	Milk	[114]
Electrochemical (DPV)	NOR	Non-invasive label-free detection based on nY <sub>2</sub> O <sub>3</sub> -CH composite	1.236 pg/mL	0.319 pg/mL–3.193 µg/mL	10 min	Spiked urine	[94]
Electrochemical (DPV)	NOR	PAMAM dendrimer encapsulated gold	0.387 ng/mL	1.0 ng/mL–10 µg/mL	50 min	Spiked animal derived food	[115]
Electrochemical (CV)	OFL	Polypyrrole film-gold nanocluster as matrix for multi-enzyme-antibody functionalized gold nanorod	0.03 ng/mL	0.08–410 ng/mL	~40 min	Buffer	[116]

Table 2. Cont.

Transducer	Target	Working Principle	LOD	Linear Range	Response Time	Medium	Reference
Electrochemical (CV)	OFL (S-OFL & R-OFL)	Dual amplification using multiwall carbon nanotubes-poly(L-lysine) for AG immobilization/multi-enzyme-labeled gold nanoflower as label	0.15 ng/mL (S-OFL) 0.30 ng/mL (R-OFL)	0.26–25.6 ng/mL (S-OFL) 0.37–12.8 ng/mL (R-OFL)	60 min	Buffer	[117]
Electrochemical	ENRO, NOR	Family selective detection using antibody functionalized CNTs	NOR: 3.2 ng/mL ENRO: 3.6 ng/mL	/	/	Antibiotic solution	[118]
Piezoelectric	CIPR	Magnetic carbon nanocomposite	2 ng/mL	5–400 ng/mL	/	Milk, meat	[100]

**Abbreviations:** NOR, norfloxacin; ENR, enrofloxacin; CIPR, ciprofloxacin; OFL, ofloxacin; UCNPs, upconversion nanoparticles; FRET, fluorescence resonance energy transfer; FQs, fluoroquinolones; AuNPs, gold nanoparticles; mab, monoclonal antibody; ICA, immunochromatographic assay; SERS, surface enhanced Raman spectroscopy; MICA, microsphere immunochromatographic assay; QICA, quantum dots immunochromatographic assay; SPCE, screen printed carbon electrode; EDC, 1-ethyl-3-(3-dimethylaminopropyl)carbodiimide; NHS, thanolamine, N-hydroxysuccinimide; BSA, bovine serum albumin; APTES, (3-amino-propyl) trimethoxysilane; ITO, indium tin oxide; CNTs, carbon nanotubes; CV, cyclic voltammetry; DPV, differential pulse voltammetry; EIS, electrochemical impedance spectroscopy. Some LOD and linear range values were converted from molarity to g/mL for better comparison.

## 2.2. Aptasensors Used for Quinolone Detection

Aptamers are short, single-stranded oligonucleotides that possess high affinity and specificity for binding ligands [119–121]. Their excellent binding properties to target analytes have led to them being referred to as “chemical antibodies” [120,122]. Aptamers are synthesized in a process termed Systematic Evolution of Ligands by Exponential Enrichment (SELEX) pioneered by Tuerk and Gold in 1990 [123]. Through repeated in vitro selection and amplification for a target analyte, large pools of random oligonucleotides evolve over time to contain highly specific aptamers [121]. Due to their unparalleled stability and ease of modification, they have gained increasing acceptance to be used as a biorecognition element in biosensors. Table 3 represents a summary of aptasensors used for quinolone detection and compares them in terms of target, detection strategy, transducer, limit of detection (LOD), linear range, response time, and sample type.

In 2019, Zhiyu et al. developed an optical aptasensor based on two interesting fields of research: gold nanoparticles (AuNPs) and Rhodamine B [124]. AuNPs are used in a variety of different fields ranging from chemistry to physics over to medicine and life science and are well-known for their inert nature, biocompatibility, and low toxicity [125]. In the field of biosensors, AuNPs are especially recognized for their unique geometrical, optical, and electrical properties [124,126].

Rhodamine B (RB) is a dye with a high absorption coefficient and broad fluorescence that is often used for fluorescent determination [124,127].

By combining AuNPs and Rhodamine B in a creative way, Zhiyu and colleagues developed a fluorescent aptasensor that was able to detect ofloxacin down to 0.6 ng/mL with a linear range of 7.23–108.41 ng/mL [124]. The aptasensor builds on the principle that dispersed AuNPs reduce the fluorescence of Rhodamine B while aggregated AuNPs do not. Using aptamers, the presence of ofloxacin causes the aggregation of AuNPs, and changes in fluorescence activity can be translated to accurately determine the antibiotic concentrations. The sensor has also been successfully tested in milk, where the LOD was calculated to be 1.3 ng/mL [124].

Based on electrochemical transduction, Taghdisi et al. developed a novel approach allowing for ultrasensitive detection of ciprofloxacin [128]. Their proposed electrochemical system consists of complementary strands of aptamer (CSs) and a double labelled aptamer with methylene blue (MB-Apt-MB) as the probe. Aided by CSs, the aptamers stay in

close contact with the electrode and a current response caused by MB can be measured. Upon the addition of the quinolone ciprofloxacin, the double labelled aptamers undergo conformational changes and the complementary strands dissociate, causing a decrease in current that can be detected. Within an hour of incubation, they achieved ultra-low detection limits of ciprofloxacin of 33.14 pg/mL with an outstanding linear detection range of 0.099–149.106 ng/mL [128]. The proposed sensor has also effectively been tested in spiked real samples like tap water, human serum, and milk, further underlining its practicability in the health and environment sectors [128].

Despite the various benefits that metallic nanoparticles bring, they tend to form conglomerates, which reduces their applicability [129–131]. To counteract this trend, so-called capping agents stabilize the interface where nanoparticles interact and therefore prevent unwanted effects. These mainly include surfactants, small ligands, polymers, cyclodextrins, and ultimately, dendrimers [130].

Dendrimers are hyperbranched nanosized structures with radial symmetry [132]. Special properties allow them to encapsulate and stabilize nanoparticles, paving the way for novel innovations in the biosensing industry [129].

As an example, Mahmoudpour et al. established an innovative apta-platform for the electroanalysis of ciprofloxacin based on poly (amidoamine) (PAMAM) dendrimer-encapsulated gold nanoparticles (Au-PAMAM) [129]. This 3D-framework has been electrodeposited on a glassy carbon electrode prior lined with reduced graphene, followed by functionalization with ciprofloxacin specific aptamers. Following 30 min of incubation with ciprofloxacin solutions of varying concentrations, DPV unveiled an extensive linear range of 0.331–331.346 ng/mL and a LOD of 33.14 pg/mL for the antibiotic [129].

Aptasensors, in conjunction with innovative research, have the ability to push the boundaries of biosensing to newfound limits. A recent publication from Wang et al. exemplified this with a sensor developed to detect different antibiotics including the quinolone enrofloxacin at 6.07 fg/mL [133]. The sensor architecture featured a novel covalent organic framework (COF) synthesized by the condensation of 1,3,6,8-tetrakis(4-formylphenyl)pyrene and melamine through imine bonds for the first time. The scaffold offered valuable properties such as rich functional groups, a large surface area, and pore cavities, causing larger quantities of aptamer strands to be immobilized. Using EIS as the method of choice, femtomolar detection limits of the antibiotic enrofloxacin and narrow linear ranges of 0.01–2 ng/mL could be achieved. Apart from that, the sensor showed good stability and acceptable applicability in human serum samples [133].

Finally, a photoelectrochemical aptasensor for the simultaneous detection of enrofloxacin and ciprofloxacin was designed by Zhang and colleagues in 2021 [134]. Photoelectrochemical (PEC) materials have become increasingly important on the rapidly progressing front of biosensor development. PEC aptasensors offer a variety of benefits over conventional sensing approaches including fast response times and improved target affinity [134]. In their publication, they synthesized two materials with excellent PEC performance: three-dimensional nitrogen-doped graphene-loaded copper indium disulfide ( $\text{CuInS}_2/3\text{DNG}$ ) and  $\text{Bi}^{3+}$ -doped black anatase titania nanoparticles decorated with reduced graphene oxide ( $\text{Bi}_3^+/\text{B-TiO}_2/\text{rGO}$ ) [134,135].

Zhang et al. deposited the two PEC materials onto circular areas distinct from each, located on an indium tin oxide electrode that was consequently functionalized with aptamers against enrofloxacin and ciprofloxacin [134]. The cathodic current generated by  $\text{CuInS}_2/3\text{DNG}$  and the anodic current generated by  $\text{Bi}_3^+/\text{B-TiO}_2/\text{rGO}$  could clearly be distinguished, which realized the dual detection of both enrofloxacin and ciprofloxacin. Zhang et al. reported wide linear ranges of 0.01 ng/mL–10,000 ng/mL for enrofloxacin and 0.01 ng/mL–1000 ng/mL for ciprofloxacin. The LOD for both antibiotics was determined as 3.3 pg/mL [134]. Moreover, they reported an optimized assay time of 40 min [134].

**Table 3.** Aptasensors for quinolone detection.

Transducer	Target	Working Principle	LOD	Linear Range	Response Time	Medium	Reference
Optical	ENRO	Aptamer-functionalized magnetic Fe <sub>3</sub> O <sub>4</sub> conjugated with UCNPs	0.06 ng/mL	1–10 ng/mL	30 min	Fish	[136]
Optical	ENRO	Label-free assay based on specific aptamers GO	1.33 ng/mL	1.8–89.85 ng/mL	30 min	Milk	[137]
Optical	ENRO	Hybrid probe based on double recognition of aptamer-MIP grafted on UCNPs	0.04 ng/mL	0.5–10 ng/mL	/	Fish	[138]
Optical	OFL	Colloidal dispersed gold nanoparticles	1.229 ng/mL	7.23–108.41 ng/mL	/	Tap water, urine	[139]
Optical	OFL	Aggregation of gold nanoparticles and quenching of fluorescence of Rhodamine B	0.6 ng/mL (water) 1.3 ng/mL (milk)	7.23–108.41 ng/mL	/	Water, milk	[124]
Optical	CIPR	Aptamer functionalized gold nanoparticles with enzyme-like activity	0.43 ng/mL (water) 0.86 ng/mL (serum) 1.06 ng/mL (milk)	1.33–165.67 ng/mL	45 min	Water, serum, milk	[140]
Electrochemical (CV, DPV)	CIPR	SPCE modified with CNTs V <sub>2</sub> O <sub>5</sub> -chitosan-composites	0.5 ng/mL	0.5–8 ng/mL	3 h	Milk	[141]
Electrochemical (DPV)	CIPR	Aptamers and SBP for access of redox probe to surface of gold electrode	0.087 ng/mL	0.265–132.54 ng/mL	<1 h	Milk, serum	[142]
Electrochemical (DPV)	CIPR	Pencil graphite electrode modified with polypyrrole, SWCNTs	1.325 ng/mL	/	/	Drugs, urine	[143]
Electrochemical (CV, DPV)	CIPR	DNA-modified GCE	38.77 ng/mL	0.331–3.313 µg/mL	/	Drugs	[144]
Electrochemical	CIPR	Reduced graphene oxide and nanogold-functionalized poly(amidoamine) dendrimer	0.331 ng/mL	0.331–331.346 ng/mL	30 min	Raw milk	[129]
Electrochemical (EIS, CV)	ENR	Novel Py-M-COF	6.07 fg/mL	0.01–2 ng/mL	/	Human serum	[133]
Electrochemical (DPV)	OFL	Gold nanoparticle coated GCE	0.361 ng/mL	18.07 ng/mL–7.23 µg/mL	2 h	Water, plant sewage	[145]
Electrochemical (DPV)	CIPR, OFL	Modified gold electrode with gold-cysteine matrix	/	/	2 h	Hospital effluent	[146]
Electrochemical (CV)	CIPR, OFL, LEV	Double-labelled aptamer to surpass complementary strand lying flat, methylene blue as redox agent	33.14 pg/mL (CIPR)	0.099–149.106 ng/mL	60 min	Human serum, milk, water	[128]

Table 3. Cont.

Transducer	Target	Working Principle	LOD	Linear Range	Response Time	Medium	Reference
Photoelectrochemical	ENR, CIPR	CuInS <sub>2</sub> /3DNG and Bi <sub>3</sub> <sup>+</sup> /B-TiO <sub>2</sub> /rGO on ITO electrode	3.3 pg/mL	ENR: 0.01–10,000 ng/mL CIP: 0.01–1000 ng/mL	40 min	Milk	[134]
Photoelectrochemical	CIPR	Ti <sub>3</sub> C <sub>2</sub> /Bi <sub>4</sub> VO <sub>8</sub> Br/TiO <sub>2</sub> nanocomposite	0.099 ng/mL	0.331–497.019 ng/mL	40 min	Milk	[147]

**Abbreviations:** NOR, norfloxacin; ENRO, enrofloxacin; CIPR, ciprofloxacin; OFL, ofloxacin; LEV, levofloxacin; CV, cyclic voltammetry; DPV, differential pulse voltammetry; EIS, electrochemical impedance spectroscopy; UCPNs, upconversion nanoparticles; GO, graphene oxide; MIP, molecular imprinted polymer; SPCE, screen printed carbon electrode; CNTs, carbon nanotubes; GCE, glassy carbon electrode; SBP, single strand binding protein; SWCNTs, single wall carbon nanotubes; Py-M-COF, covalent organic framework by condensation polymerization of 1,3,6,8-tetrakis(4-formylphenyl)pyrene and melamine through imine bonds; DNA, desoxyribonucleic acid; ITO, indium tin oxide; CuInS<sub>2</sub>/3DNG, three-dimensional nitrogen-doped graphene-loaded copper indium disulfide; Bi<sub>3</sub><sup>+</sup>/B-TiO<sub>2</sub>, Bi<sub>3</sub><sup>+</sup>-doped black anatase titania nanoparticles decorated with reduced graphene oxide; rGO, reduced graphene oxide. Some LOD and linear range values were converted from molarity to g/mL for better comparison.

### 2.3. Enzymatic Biosensors for Quinolone Detection

Enzymes are attractive candidates for use as biorecognition elements or signal amplifiers in biosensors due to their strong enzyme–substrate interactions and high turnover rates. These interactions can result in changes such as proton concentration or light emission, which can then be detected and translated into measurable signals by transducers [148]. The detection of environmental pollutants with sensors using such enzymes represents a promising field of research [149]. Despite being underrepresented in the field of quinolone detection, enzyme-based biosensors have the potential to be highly effective in this area. The following section will review selected publications reporting enzymatic sensors for quinolone detection. In Table 4, they are compared in terms of the target analyte, limit of detection, linear detection range, response time, and operating media.

Oxidative enzymes such as tyrosinases or laccases have recently gained popularity due to their versatile and potent analyte recognition [149]. To quantify pipemidic acid (PA), a synthetic quinolone, Bertolino et al. developed a microfluidic-enzymatic electrochemical sensor [150]. The sensor is based on the tyrosinase enzyme immobilized on 3-aminopropyl-modified-controlled-pore glass (APCPG). Tyrosinase is known to catalyze the oxidation of catechol to o-benzoquinone. PA then undergoes a reaction with o-benzoquinone, a reduction that can be measured in a change in peak current against a gold electrode. Using this innovative enzymatic biosensor, Bertolino et al. were able to detect PA concentrations as low as 5.46 ng/mL and a linear range from 0.006 µg/mL to 21.2 µg/mL could be achieved. Furthermore, the research team conducted studies regarding the long-term stability of the enzymatic system: By injecting a standard into the microfluidic system after samples were run, they showed that no decay of current could be observed after six samples [150].

In 2020, Esen et al. developed a novel approach for inhibition-based enzymatic sensors. For the first time, they reported a fluorescence assay for the detection of ciprofloxacin based on the enzymes paraoxonase (PO) and laccase (Lac) immobilized on anthracene-sequestered polyamic acid films [151]. POs belong to the enzyme family of esterases and cleave ester bonds of a broad range of targets [151,152]. In this study, PO catalyzed the reaction of phenyl acetate to acetic acid and phenol. This is where Lac takes over and further oxidizes the phenol, a process fueled by oxygen consumption. Molecular oxygen quenches the fluorescence of anthracene, resulting in increased fluorescence upon phenol oxidation. Consequently, ciprofloxacin was introduced to the fine-tuned pH adjusted system and a calibration curve based on the observed decrease in fluorescence emission was established. Using this inexpensive, non-competitive enzyme assay, Esen et al. determined the limit of detection to be 3.313 µg/mL, and the linear detection ranged from 6.63 to 165.67 ng/mL. To our current understanding, this system represents the swiftest method for detecting quinolones at low concentrations, achieving a response time of just 2 min [151].

Another example of enzyme-based sensors developed to detect quinolone antibiotics is a study from Torriero et al., where they achieved a limit of detection of 0.099 ng/mL and 0.096 ng/mL for ciprofloxacin and norfloxacin, respectively [153]. The proposed biosensor acts on the principle that horseradish peroxidase (HRP), immobilized on a rotating disk, catalyzes the oxidation of catechol in the presence of hydrogen peroxide. Catechol can undergo reversible electrooxidation when exposed to specific potentials, resulting in a change in current. The two quinolones used in this study, norfloxacin and ciprofloxacin, contain piperazine compounds. Due to these compounds, their introduction into the solution causes quick reactions with the catechol, resulting in a current decrease proportional to the concentration of antibiotic in the system [153].

A biomimetic strategy was employed by Cardoso et al. in a recent publication from 2021 [154]. As discussed in Chapter 1.2, one of the cellular targets of quinolone antibiotics is the enzyme DNA gyrase. In their work, they exploited this fact by attaching DNA gyrase aided by ionic interactions to a carbon support on common, screen-printed electrodes—a strategy that was addressed for the first time at the time of publication [154]. In an elaborate process, the carboxylic groups of nanotubes making up the carbon support were activated by incubation in *N*'-ethyl-*N*'-(3-dimethylaminopropyl)carbodiimide hydrochloride (EDAC) and *N*-hydroxysuccinimide (NHS) solution. Consequently, by adding *p*-phenylenediamine, an amine layer was formed on top of the nanotubes. Finally, the DNA gyrase, acting as the biorecognition element of the sensor, was added to the construct. Upon addition of either ciprofloxacin or norfloxacin, the electrochemical changes were monitored and translated to the exact concentration of the antibiotics. The sensor showed an excellent performance, with LODs of 1 ng/mL (CIPR) and 9.64 ng/mL (NOR). They reported a broad linear detection rate of 10 ng/mL–100 µg/mL for ciprofloxacin and a narrower range of 9.64 ng/mL–9.65 µg/mL for norfloxacin [154]. Moreover, Cardoso and colleagues demonstrated a response rate of the sensor of 30 min. With this novel biomimetic approach, Cardoso et al. opened the door to various creative enzyme-based quinolone sensors in the future.

In a most recent publication from 2023, Yan and colleagues developed an enzymatic biosensor for the detection of quinolones based on Cu<sup>2+</sup>-modulated signal amplification [155]. Quinolones possess an affinity for copper cations and readily form complexes with them [155,156]. This in turn inhibits the DNAzyme, an enzyme that is dependent on copper cations for proper function. A DNA probe on the surface of the electrode can then undergo a hybridization chain reaction, resulting in long DNA wires, which leads to signal amplification directly proportional to quinolone concentration. For ciprofloxacin, Yan et al. reported a limit of detection of 0.052 ng/mL and a linear detection rate of 0.1–200 ng/mL [155]. This sensor is, to the best of our knowledge, one of the first enzymatic biosensors demonstrated to detect quinolones not only in buffers, but also in foodstuff samples such as milk.

Enzymes can also be used as electrochemical detection labels to amplify signals in various kinds of biosensors. Based on a sandwich immunoreaction alongside innovative nanomaterials, Zang and colleagues manufactured an electrochemical immunosensor to detect trace amounts of ofloxacin [116]. Following an elaborate functionalization with a polypyrrole gold nanocluster matrix, the surface was treated with ovalbumin conjugated ofloxacin (OFL-OVA) as the competitor. Then, a mixture of primary ofloxacin antibodies and ofloxacin was added to the sensor and competition with the already bound conjugated ofloxacin took place [116]. The more ofloxacin there is in the solution to be tested, the less the antibodies will bind to the already immobilized OFL-OVA. This step was followed by introducing gold nanorods decorated with the enzyme HRP and secondary antibodies. In the end the HRP substrate hydroquinone (HQ) and H<sub>2</sub>O<sub>2</sub> was added, and CV was used to record the catalytic current. Zang and colleagues were able to detect ofloxacin down to 0.03 ng/mL while covering a broad linear range from 0.08 to 410 ng/mL. They argue that this great sensitivity was in part achieved by the usage of gold nanorods as the carrier for the HRP–antibody complex [116].

Significant differences in antibacterial activity between ofloxacin enantiomers demonstrate the need for quick, enantioselective biosensors. Two years later, the same research team developed an enantioselective electrochemical sensor able to detect ofloxacin [117]. They used multi-walled carbon nanotubes (MWCNT) and poly(L-lysine) (PLL) as the matrix and gold nanoflowers multi-labeled with HRP to greatly amplify the signal. With this innovative approach, they could distinguish between S-ofloxacin and R-ofloxacin with detection limits of 0.15 ng/mL and 0.30 ng/mL, respectively [117].

**Table 4.** Enzyme-based biosensors for quinolone detection.

Transducer	Target	Working Principle	LOD	Linear Range	Response Time	Medium	Reference
Optical	CIPR	Bienzymatic sensor (paraoxonase and laccase) immobilized on anthracene-sequestered polyamic acid films	3.313 µg/mL	6.63–165.67 ng/mL	2 min	Buffer	[151]
Electrochemical (CV)	OFL	Polypyrrole film-gold nanocluster as matrix for multi-enzyme-antibody functionalized gold nanorod	0.03 ng/mL	0.08–410 ng/mL	3 h	Buffer	[116] *
Electrochemical (V)	OFL (S-OFL & R-OFL)	Dual amplification using multiwall carbon nanotubes-poly(L-lysine) for AG immobilization/multi-enzyme-labeled gold nanoflower as the label	0.15 ng/mL (S-OFL) 0.30 ng/mL (R-OFL)	S-OFL: 0.26–25.6 ng/mL R-OFL: 0.37–12.8 ng/mL	2 h	Buffer	[117] *
Electrochemical	CIPR, NOR	Biomimetic strategy—DNA Gyrase by ionic interactions attached to a SPCE	1 ng/mL (CIPR) 9.64 ng/mL (NOR)	10 ng/mL–0.1 mg/mL (CIPR) 9.64 ng/mL– 9.65 µg/mL (NOR)	30 min	Buffer	[154]
Electrochemical (CV)	CIPR, NOR	Horseradish peroxidase immobilized on a rotating disk; reduction detected on GCE	0.099 ng/mL (CIPR) 0.096 ng/mL (NOR)	0.007–21 µg/mL (CIPR) 0.006–20.76 µg/mL (NOR)	/	Buffer	[153]
Electrochemical	CIPR	Cu <sup>2+</sup> -modulated signal amplification/DNAzyme	0.052 ng/mL	0.1 ng/mL to 200 ng/mL	~4 h	Buffer/Milk	[155]
Electrochemical	PA	Immobilized tyrosinase enzyme on APCPG	5.46 ng/mL	0.006 µg/mL– 21.2 µg/mL	/	Buffer	[150]

**Abbreviations:** CIPR, ciprofloxacin; NOR, norfloxacin, OFL, ofloxacin; pipemidic acid, PA; CV, cyclic voltammetry; DNA, deoxyribonucleic acid; SPCE, screen printed carbon electrode; GCE, glassy carbon electrode; APCPG, 3-aminopropyl-modified-controlled-pore glass. Some LOD and linear range values were converted from molarity to g/mL for better comparison. \* Sensors also use enzymes in their design but are considered immunosensors by respective authors.

### 3. Discussion and Future Implications

This review holistically summarized the body of literature of immunosensors, aptasensors, and enzymatic sensors for the detection of quinolone antibiotics.

The body of comparative experimental studies between different biosensor types is small, making it hard to directly compare sensor performances under equal settings [157].

However, when comparing antibodies and aptamers as capture probes in biosensor designs, consensus exists that aptamers possess intrinsic advantages over antibodies: they are known to have high target affinity, a robust, animal-free production, and are easy to chemically modify. Thus, they have become the most promising alternative to antibodies in the development of biosensors [121,158]. Nonetheless, antibodies should not be neglected, as they still represent the first choice for biorecognition elements in biosensors [121].

Enzymatic sensors represent yet another field of research in the development of biosensors. The blood glucose monitor represents a famous example of an enzyme-based sensor that has been commercialized [159]. Notwithstanding their benefits such as high specificity and sensitivity, a major limitation is possible interference from chemicals in the sample matrix. Enzymes are delicate machineries often requiring specific environmental parameters to function properly. Efforts to mitigate endogenous interference by incorporating nanomaterials and matrices to stabilize the enzyme are being made [148].

Regarding the different types of developed quinolone sensors, the following conclusions can be drawn: the response time of most immuno- and aptasensors lies between 10 and 60 min. This is due to the necessary incubation steps of the target analyte with the biorecognition element of the sensor. Notably, from the sensors summarized in this paper, immunosensors appear to populate the lower part of this range, while aptasensors tend to take longer on average. However, the fastest response time of quinolone detection was achieved by, to the best of our knowledge, Esen and colleagues in 2020. With their flexible bienzymatic system, they monitored ciprofloxacin at minute levels in buffer samples [151]. Unfortunately, no stability experiments have been performed.

The sensor with the lowest level of successful quinolone detection is an aptasensor developed by Wang et al., reaching femtomolar ranges [133]. Although showing a remarkable performance, the linear range was narrow, making the sensor more of a specialist than a generalist. In general, aptasensors appear to be slightly more sensitive than antibody and enzyme-based sensors. However, Arshavsky-Graham et al. explained that both aptamers and antibody performance mainly depends, more than anything else, on proper integration within the sensing interface, making it difficult to compare them with each other and to draw informed conclusions [157].

Future efforts should be focused on bringing sensor technologies from the laboratory to the field. The biosensors discussed in this review performed excellently, but the step toward field testing has yet to be made. Efforts should be directed to increase portability, point-of-care detection, and ease-of-use for non-professionals in technologically challenged areas. Thus, it is crucial to assess sensor stability over time as an important criterion when assessing the performance of biosensors. In this regard, Cheng et al. paved the way for future research by introducing a portable and digitalized system for quinolone detection that was shown to be relatively stable for up to 4 weeks [89]. It is worth noting that there has been limited focus on sensor stability in biosensor studies. Among the few that have examined stability, the achieved durations ranged from a few days up to a maximum of 4 weeks at either 4 degrees or at room temperature [81,89,90,94,114–117,129,133,134,141,145,150]. Most studies concluded their stability testing after a 4-week period despite the sensor's continued relatively strong performance. We therefore consider it necessary to place emphasis on research that is aimed to increase the sensor lifetime and perform comprehensive long-term stability studies spanning many months.

The sensors presented in this review were shown to measure quinolones across different media. Thus, it is essential to probe for possible matrix interference in complex samples when developing biosensors. Zhang et al. addressed this issue by conducting several interference experiments [109]. Since it was their goal to ultimately detect quinolones in environmental samples such as tap pond or river water, the effects of parameters such as pH and salinity on sensor performance were evaluated. They found that their assay was stable across a broad pH range and high concentrations of heavy metals. However, the addition of  $Mg^{2+}$  ions led to interference of the signal. To combat ions, they added EDTA, a chelating agent, but above a certain concentration, the cations could not be removed from

the system any longer. They argued that this was due to the unwanted aggregation of gold nanoparticles [109,160]. Conversely, studies from Chen et al. and Lamarca et al. could not evaluate any interference effects from water samples for their respective sensors [89,110].

Pinacho and colleagues discussed the milk matrix effect in their biosensor paper. Due to milk being a complex matrix composed of fat protein, sugars, and minerals, the interaction between the biorecognition element and the target analyte can be mitigated [113,161]. In two studies from Sheng et al. and Taranova et al., the matrix effects could be removed via high dilution of supernatants extracted from animal tissues and milk samples, respectively [105,107].

Standard methods for the determination of antibiotic residues in the environment include HPLC or MS-HPLC, but the need for supporting infrastructure and their lack of portability does not make them a good fit for field testing [162]. Due to their innate ability to deliver rapid results while staying portable, biosensors present a natural fit to overcome such limitations. However, at present, standardized schemes for rapid detection using biosensors are lacking. To integrate biosensors into existing regulatory frameworks to establish them as an integral part of environmental antibiotic monitoring and food safety, the need for improved biosensors specifically for field testing is great.

To make biosensors more portable, applicable outside of the laboratory, and easier to use, a fine balance must be found between implementing these points and simpler sensor architectures.

Many biosensors demonstrate ultrasensitive detection of quinolone antibiotics, but high performance often comes with complex sensor design and functionalization protocols. Sometimes, ultrasensitive methods are not needed, and a decrease in performance could improve the design in terms of simplicity. This would positively impact development toward portability and field-testing. A simpler sensor architecture and protocol of functionalization would also pave the way for future automation. This would enable faster upscaling and commercialization of the product to make them globally available.

In addition, this review identified new trends in recent publications on quinolone detection that suggest interesting directions for the future.

Although enzymatic biosensors are underrepresented in the field of quinolone detection, biomimetics, an exceptional strategy published by Cardoso and colleagues, opens the door for countless innovations to come [154]. Their strategy of mimicking the natural target of quinolone antibiotics, the enzyme DNA gyrase, could be applied to various other analytes. This approach could allow for the detection of whole families of antibiotics and presents an intriguing direction worth exploring.

The use of nanotechnology has significantly impacted the biosensor industry. Rare earth metal-based nanoparticles offer various advantages when compared to other materials used for biomedical purposes including low toxicity and high chemical stability [91]. They are being used in various biomedical applications including drug delivery, bioimaging, and ultimately, biosensing [91]. In the detection of quinolones with biosensors, there has been a clear trend toward the use of rare earth metals as nanomaterials, further pointing out their importance now and for future research [90,94,101,109].

So-called capping agents are often utilized to prevent the formation of conglomerates and the overgrowth of nanoparticles [130,131]. Mahmoudpour et al. made use of a capping agent and claimed that it expanded the surface area with the target while improving the electrochemical properties to better interact with the analyte of interest [129]. However, capping agents can also exhibit “poisonous” effects, limiting the accessibility of active sites [163]. The incorporation of nanoparticles into biosensors already offers a variety of benefits and an improved nanotechnological understanding of capping agents could not only greatly benefit the future of quinolone detection, but also biosensing as a whole.

Finally, a noteworthy observation has been made not only concerning quinolone sensors but also in relation to general biosensing applications. In the wake of climate change, the need for reusable sensors is greater than ever. Many sensing interfaces are difficult to regenerate after being used, limiting most sensors to a single-use type [164].

Future research dedicated to this issue would save on material and production costs while minimizing the negative environmental impact. Efforts have been made to produce nanoparticles in an eco-compliant manner: “green synthesis” has received considerable attention as an eco-friendly and sustainable emerging protocol [165,166].

Quinolone biosensors have an undeniable impact on our society in terms of the detection of analytes, especially in the environmental and health sectors. With the global emergence of resistant microbes, biosensors have surfaced as a promising tool to counteract this issue by allowing for rapid and sensitive detection of antibiotics. The papers presented in this review lay important groundwork for our future. It is now important to build on and expand these great novelties to work on essential future innovations: increased portability and point-of-care detection while maintaining sufficient performance and ease of use, increased research on biomimetic strategies, rare earths as nanomaterials, capping agents, and ultimately, the realization of environmentally friendly solutions.

**Author Contributions:** Conceptualization, F.T. and F.A.A.; formal analysis, F.T.; investigation, F.T.; writing—original draft preparation, F.T.; writing—review and editing, F.A.A. and F.T.; visualization, F.T.; supervision, F.A.A.; project administration, F.A.A.; funding acquisition, F.A.A. All authors have read and agreed to the published version of the manuscript.

**Funding:** This work was supported by the European Regional Development Fund.

**Institutional Review Board Statement:** Not applicable.

**Informed Consent Statement:** Not applicable.

**Data Availability Statement:** Data sharing not applicable. No new data were created or analyzed in this study. Data sharing is not applicable to this article.

**Conflicts of Interest:** The authors declare no conflict of interest.

## References

1. Urban-Chmiel, R.; Marek, A.; Stepien-Pysniak, D.; Wieczorek, K.; Dec, M.; Nowaczek, A.; Osek, J. Antibiotic Resistance in Bacteria—A Review. *Antibiotics* **2022**, *11*, 1079. [[CrossRef](#)]
2. Pauter, K.; Szultka-Młyńska, M.; Buszewski, B. Determination and Identification of Antibiotic Drugs and Bacterial Strains in Biological Samples. *Molecules* **2020**, *25*, 2556. [[CrossRef](#)]
3. Ahmed, S.; Ning, J.; Peng, D.; Chen, T.; Ahmad, I.; Ali, A.; Lei, Z.; Abu bakr Shabbir, M.; Cheng, G.; Yuan, Z. Current advances in immunoassays for the detection of antibiotics residues: A review. *Food Agric. Immunol.* **2020**, *31*, 268–290. [[CrossRef](#)]
4. Zhang, Z.; Cheng, H. Recent Development in Sample Preparation and Analytical Techniques for Determination of Quinolone Residues in Food Products. *Crit. Rev. Anal. Chem.* **2017**, *47*, 223–250. [[CrossRef](#)]
5. Jin, Y.; Dou, M.; Zhuo, S.; Li, Q.; Wang, F.; Li, J. Advances in microfluidic analysis of residual antibiotics in food. *Food Control* **2022**, *136*, 108885. [[CrossRef](#)]
6. Haleem, A.; Javaid, M.; Singh, R.P.; Suman, R.; Rab, S. Biosensors applications in medical field: A brief review. *Sens. Int.* **2021**, *2*, 100100. [[CrossRef](#)]
7. Gavrila, S.; Ștefan Ursachi, C.; Per, S.; Munteanu, F.D. Recent Trends in Biosensors for Environmental Quality Monitoring. *Sensors* **2022**, *22*, 1513. [[CrossRef](#)] [[PubMed](#)]
8. Curulli, A. Electrochemical Biosensors in Food Safety: Challenges and Perspectives. *Molecules* **2021**, *26*, 2940. [[CrossRef](#)]
9. Yang, Z.; Zhang, X.; Guo, J. Functionalized Carbon-Based Electrochemical Sensors for Food and Alcoholic Beverage Safety. *Appl. Sci.* **2022**, *12*, 9082. [[CrossRef](#)]
10. Liu, H.; Mulholland, S.G. Appropriate antibiotic treatment of genitourinary infections in hospitalized patients. *Am. J. Med.* **2005**, *118*, 14–20. [[CrossRef](#)] [[PubMed](#)]
11. Pham, T.D.M.; Ziora, Z.M.; Blaskovich, M.A.T. Quinolone antibiotics. *MedChemComm* **2019**, *10*, 1719–1739. [[CrossRef](#)] [[PubMed](#)]
12. Turnidge, J. Pharmacokinetics and Pharmacodynamics of Fluoroquinolones. *Drugs* **1999**, *58*, 29–36. [[CrossRef](#)] [[PubMed](#)]
13. Wang, Q.; Xue, Q.; Chen, T.; Li, J.; Liu, Y.; Shan, X.; Liu, F.; Jia, J. Recent advances in electrochemical sensors for antibiotics and their applications. *Chin. Chem. Lett.* **2020**, *32*, 609–619. [[CrossRef](#)]
14. Pollap, A.; Kochana, J. Electrochemical Immunosensors for Antibiotic Detection. *Biosensors* **2019**, *9*, 61. [[CrossRef](#)]
15. Mehlhorn, A.; Rahimi, P.; Joseph, Y. Aptamer-Based Biosensors for Antibiotic Detection: A Review. *Biosensors* **2018**, *8*, 54. [[CrossRef](#)]
16. Jiwanti, P.K.; Wardhana, B.Y.; Sutanto, L.G.; Chanif, M.F. A Review on Carbon-based Electrodes for Electrochemical Sensor of Quinolone Antibiotics. *ChemistrySelect* **2022**, *7*, e202103997. [[CrossRef](#)]

17. Majdinasab, M.; Mitsubayashi, K.; Marty, J.L. Optical and Electrochemical Sensors and Biosensors for the Detection of Quinolones. *Rends Biotechnol.* **2019**, *37*, 898–915. [CrossRef]
18. Ansari, M.J.; Bokov, D.O.; Jasim, S.A.; Rudiansyah, M.; Suksatan, W.; Yasin, G.; Chupradit, S.; Alkaim, A.F.; Mustafa, Y.F.; Tarek, D.I. Emerging optical and electrochemical biosensing approaches for detection of ciprofloxacin residues in food and environment samples: A comprehensive overview. *J. Mol. Liq.* **2022**, *354*, 118895. [CrossRef]
19. Liu, C.; Tan, L.; Zhang, L.; Tian, W.; Ma, L. A Review of the Distribution of Antibiotics in Water in Different Regions of China and Current Antibiotic Degradation Pathways. *Front. Environ. Sci.* **2021**, *9*, 692298. [CrossRef]
20. Polianciuc, S.I.; Gurzău, A.E.; Kiss, B.; Ștefan, M.G.; Loghin, F. Antibiotics in the environment: Causes and consequences. *Med. Pharm. Rep.* **2020**, *93*, 231–240. [CrossRef]
21. Antibioticsfinder. Available online: <https://www.antibioticsfinder.com/antibioticsfinder> (accessed on 25 August 2023).
22. OIE List of Antimicrobial Agents of Veterinary Importance. Available online: <https://www.woah.org/app/uploads/2021/06/a-oie-list-antimicrobials-june2021.pdf> (accessed on 4 September 2023).
23. Appelbaum, P.C.; Hunter, P.A. The fluoroquinolone antibacterials: Past, present and future perspectives. *Int. J. Antimicrob. Agents* **2000**, *16*, 5–15. [CrossRef]
24. Emmerson, A.M. The quinolones: Decades of development and use. *J. Antimicrob. Chemother.* **2003**, *51*, 13–20. [CrossRef]
25. Wagenlehner, F.M.E.; Naber, K.G. Fluoroquinolone antimicrobial agents in the treatment of prostatitis and recurrent urinary tract infections in men. *Curr. Infect. Dis. Rep.* **2005**, *7*, 9–16. [CrossRef]
26. Pommier, Y.; Leo, E.; Zhang, H.; Marchand, C. DNA topoisomerases and their poisoning by anticancer and antibacterial drugs. *Chem. Biol.* **2010**, *17*, 421–433. [CrossRef]
27. Champoux, J.J. DNA Topoisomerases: Structure, Function, and Mechanism. *Ann. Rev. Biochem.* **2001**, *70*, 369–413. [CrossRef]
28. Levine, C.; Hiasa, H.; Mariani, K.J. DNA gyrase and topoisomerase IV: Biochemical activities, physiological roles during chromosome replication, and drug sensitivities. *Biochim. Et Biophys. Acta (BBA) Gene Struct. Expr.* **1998**, *1400*, 29–43. [CrossRef]
29. Wang, J.C. DNA Topoisomerases. *Ann. Rev. Biochem.* **1985**, *54*, 665–697. [CrossRef] [PubMed]
30. Gellert, M.; Mizuuchi, K.; O’Dea, M.H.; Nash, H.A. DNA gyrase: An enzyme that introduces superhelical turns into DNA. *Proc. Natl. Acad. Sci. USA* **1976**, *73*, 3872–3876. [CrossRef] [PubMed]
31. Sutormin, D.A.; Galivondzhyan, A.K.; Polkhovskiy, A.V.; Kamalyan, S.O.; Severinov, K.V.; Dubiley, S.A. Diversity and Functions of Type II Topoisomerases. *Acta Naturae* **2021**, *13*, 59–75. [CrossRef]
32. Forterre, P.; Gribaldo, S.; Gabelle, D.; Serre, M.-C. Origin and evolution of DNA topoisomerases. *Biochimie* **2007**, *89*, 427–446. [CrossRef]
33. Anderson, V.; Osherooff, N. Type II Topoisomerases as Targets for Quinolone Antibacterials Turning Dr. Jekyll into Mr. Hyde. *Curr. Pharm. Des.* **2001**, *7*, 337–353. [CrossRef] [PubMed]
34. Deweese, J.E.; Osherooff, N. The DNA cleavage reaction of topoisomerase II: Wolf in sheep’s clothing. *Nucleic Acids Res.* **2008**, *37*, 738–748. [CrossRef] [PubMed]
35. Aldred, K.J.; Kerns, R.J.; Osherooff, N. Mechanism of quinolone action and resistance. *Biochemistry* **2014**, *53*, 1565–1574. [CrossRef] [PubMed]
36. Drlica, K.; Hiasa, H.; Kerns, R.; Malik, M.; Mustaev, A.; Zhao, X. Quinolones: Action and resistance updated. *Curr. Top. Med. Chem.* **2009**, *9*, 981–998. [CrossRef] [PubMed]
37. Zaman, S.B.; Hussain, M.A.; Nye, R.; Mehta, V.; Mamun, K.T.; Hossain, N. A Review on Antibiotic Resistance: Alarm Bells are Ringing. *Cureus* **2017**, *9*, e1403. [CrossRef] [PubMed]
38. Antimicrobial Resistance Collaborators. Global burden of bacterial antimicrobial resistance in 2019: A systematic analysis. *Lancet* **2022**, *399*, 629–655. [CrossRef]
39. Deku, J.G.; Duedu, K.O.; Ativi, E.; Kpene, G.E.; Feglo, P.K. Occurrence and distribution of extended-spectrum  $\beta$ -lactamase in clinical *Escherichia coli* isolates at Ho Teaching Hospital in Ghana. *Ghana Med. J.* **2021**, *55*, 298–307. [CrossRef]
40. Hooper, D.C.; Jacoby, G.A. Mechanisms of drug resistance: Quinolone resistance. *Ann. N. Y. Acad. Sci.* **2015**, *1354*, 12–31. [CrossRef]
41. Yoshida, H.; Bogaki, M.; Nakamura, M.; Nakamura, S. Quinolone resistance-determining region in the DNA gyrase *gyrA* gene of *Escherichia coli*. *Antimicrob. Agents Chemother.* **1990**, *34*, 1271–1272. [CrossRef]
42. Yoshida, H.; Bogaki, M.; Nakamura, M.; Yamanaka, L.M.; Nakamura, S. Quinolone resistance-determining region in the DNA gyrase *gyrB* gene of *Escherichia coli*. *Antimicrob. Agents Chemother.* **1991**, *35*, 1647–1650. [CrossRef]
43. Breines, D.M.; Ouabdesselam, S.; Ng, E.Y.; Tankovic, J.; Shah, S.; Soussy, C.J.; Hooper, D.C. Quinolone resistance locus *nfxD* of *Escherichia coli* is a mutant allele of the *parE* gene encoding a subunit of topoisomerase IV. *Antimicrob. Agents Chemother.* **1997**, *41*, 175–179. [CrossRef] [PubMed]
44. McMurry, L.; Petrucci, R.E., Jr.; Levy, S.B. Active efflux of tetracycline encoded by four genetically different tetracycline resistance determinants in *Escherichia coli*. *Proc. Natl. Acad. Sci. USA* **1980**, *77*, 3974–3977. [CrossRef] [PubMed]
45. Ball, P.R.; Shales, S.W.; Chopra, I. Plasmid-mediated tetracycline resistance in *Escherichia coli* involves increased efflux of the antibiotic. *Biochem. Biophys. Res. Commun.* **1980**, *93*, 74–81. [CrossRef] [PubMed]
46. Poole, K. Efflux-mediated resistance to fluoroquinolones in gram-negative bacteria. *Antimicrob. Agents Chemother.* **2000**, *44*, 2233–2241. [CrossRef]

47. Schindler, B.D.; Frempong-Manso, E.; DeMarco, C.; Kosmidis, C.; Matta, V.; Seo, S.; Kaatz, G. Analyses of multidrug efflux pump-like proteins encoded on the *Staphylococcus aureus* chromosome. *Antimicrob. Agents Chemother.* **2015**, *59*, 747–748. [[CrossRef](#)]
48. Patel, K.N.; Patel, J.K.; Patel, M.P.; Rajput, G.C.; Patel, H.A. Introduction to hyphenated techniques and their applications in pharmacy. *Pharm. Methods* **2010**, *1*, 2–13. [[CrossRef](#)]
49. Lombardo-Agüí, M.; Cruces-Blanco, C.; García-Campaña, A.M.; Gracia, L. Multiresidue analysis of quinolones in water by ultra-high performance liquid chromatography with tandem mass spectrometry using a simple and effective sample treatment. *J. Sep. Sci.* **2014**, *37*, 2145–2152. [[CrossRef](#)]
50. Wei, L.; Chen, Y.; Shao, D.; Li, J. Simultaneous Determination of Nine Quinolones in Pure Milk Using PFSPE-HPLC-MS/MS with PS-PAN Nanofibers as a Sorbent. *Foods* **2022**, *11*, 1843. [[CrossRef](#)]
51. Zhu, Y.; He, P.; Hu, H.; Qi, M.; Li, T.; Zhang, X.; Guo, Y.; Wu, W.; Lan, Q.; Yang, C.; et al. Determination of quinolone antibiotics in environmental water using automatic solid-phase extraction and isotope dilution ultra-performance liquid chromatography tandem mass spectrometry. *J. Chromatogr. B* **2022**, *1208*, 123390. [[CrossRef](#)]
52. Annunziata, L.; Visciano, P.; Stramenga, A.; Colagrande, M.; Campana, G.; Scortichini, G.; Migliorati, G.; Compagnone, D. Development and Validation of a Method for the Determination of Quinolones in Muscle and Eggs by Liquid Chromatography-Tandem Mass Spectrometry. *Food Anal. Methods* **2016**, *9*, 2308–2320. [[CrossRef](#)]
53. Chang, C.S.; Wang, W.H.; Tsai, C.E. Simultaneous determination of 18 quinolone residues in marine and livestock products by liquid chromatography/tandem mass spectrometry. *J. Food Drug Anal.* **2010**, *18*, 87–97. [[CrossRef](#)]
54. Cavazos-Rocha, N.; Carmona-Alvarado, I.; Vera-Cabrera, L.; Waksman-de-Torres, N.; Salazar-Cavazos, M.d.l.L. HPLC Method for the Simultaneous Analysis of Fluoroquinolones and Oxazolidinones in Plasma. *J. Chromatogr. Sci.* **2014**, *52*, 1281–1287. [[CrossRef](#)]
55. Peris-Vicente, J.; Peris-García, E.; Albiol-Chiva, J.; Durgbanshi, A.; Ochoa-Aranda, E.; Carda-Broch, S.; Bose, D.; Esteve-Romero, J. Liquid chromatography, a valuable tool in the determination of antibiotics in biological, food and environmental samples. *Microchem. J.* **2022**, *177*, 107309. [[CrossRef](#)]
56. Zhang, F.; Liu, M.; Liu, R.; Li, J.; Sang, Y.; Tang, Y.; Wang, X.; Wang, S. A broad-spectrum sensing strategy for the tetracycline family of antibiotics based on an ovalbumin-stabilized gold nanocluster and its application in a pump-free microfluidic sensing platform. *Biosens. Bioelectron.* **2020**, *171*, 112701. [[CrossRef](#)] [[PubMed](#)]
57. Zhao, M.; Li, X.; Zhang, Y.; Wang, Y.; Wang, B.; Zheng, L.; Zhang, D.; Zhuang, S. Rapid quantitative detection of chloramphenicol in milk by microfluidic immunoassay. *Food Chem.* **2020**, *339*, 127857. [[CrossRef](#)] [[PubMed](#)]
58. Sierra-Rodero, M.; Fernández-Romero, J.M.; Gómez-Hens, A. Determination of aminoglycoside antibiotics using an on-chip microfluidic device with chemiluminescence detection. *Microchim. Acta* **2012**, *179*, 185–192. [[CrossRef](#)]
59. Tang, M.; Zhao, Y.; Chen, J.; Xu, D. On-line multi-residue analysis of fluoroquinolones and amantadine based on an integrated microfluidic chip coupled to triple quadrupole mass spectrometry. *Anal. Methods* **2020**, *12*, 5322–5331. [[CrossRef](#)]
60. Pan, Y.; Yang, H.; Wen, K.; Ke, Y.; Shen, J.; Wang, Z. Current advances in immunoassays for quinolones in food and environmental samples. *TrAC Trends Anal. Chem.* **2022**, *157*, 116726. [[CrossRef](#)]
61. Wen, K.; Nölke, G.; Schillberg, S.; Wang, Z.; Zhang, S.; Wu, C.; Jiang, H.; Meng, H.; Shen, J. Improved fluoroquinolone detection in ELISA through engineering of a broad-specific single-chain variable fragment binding simultaneously to 20 fluoroquinolones. *Anal. Bioanal. Chem.* **2012**, *403*, 2771–2783. [[CrossRef](#)]
62. Huet, A.C.; Charlier, C.; Tittlemier, S.A.; Singh, G.; Benrejeb, S.; Delahaut, P. Simultaneous determination of (fluoro)quinolone antibiotics in kidney, marine products, eggs, and muscle by enzyme-linked immunosorbent assay (ELISA). *J. Agric. Food Chem.* **2006**, *54*, 2822–2827. [[CrossRef](#)]
63. Yadoung, S.; Ishimatsu, R.; Xu, Z.; Sringarm, K.; Pata, S.; Thongkham, M.; Chantara, S.; Pattarawarapan, M.; Hongsibsong, S. Development of IgY-Based Indirect Competitive ELISA for the Detection of Fluoroquinolone Residues in Chicken and Pork Samples. *Antibiotics* **2022**, *11*, 1512. [[CrossRef](#)] [[PubMed](#)]
64. Zhang, B.; Lang, Y.; Guo, B.; Cao, Z.; Cheng, J.; Cai, D.; Shentu, X.; Yu, X. Indirect Competitive Enzyme-Linked Immunosorbent Assay Based on Broad-Spectrum Antibody for Simultaneous Determination of Thirteen Fluoroquinolone Antibiotics in *Rana catesbeianus*. *Foods* **2023**, *12*, 2530. [[CrossRef](#)] [[PubMed](#)]
65. Sakamoto, S.; Putalun, W.; Vimolmangkang, S.; Phoolcharoen, W.; Shoyama, Y.; Tanaka, H.; Morimoto, S. Enzyme-linked immunosorbent assay for the quantitative/qualitative analysis of plant secondary metabolites. *J. Nat. Med.* **2018**, *72*, 32–42. [[CrossRef](#)]
66. Heineman, W.R.; Jensen, W.B. Leland C. Clark Jr. (1918–2005). *Biosens. Bioelectron.* **2006**, *21*, 1403–1404. [[CrossRef](#)]
67. Naresh, V.; Lee, N. A Review on Biosensors and Recent Development of Nanostructured Materials-Enabled Biosensors. *Sensors* **2021**, *21*, 1109. [[CrossRef](#)]
68. Dellweg, H.; Dellweg, H.; Gierasch, L.M. International union of pure and applied chemistry applied chemistry division commission on biotechnology\* glossary for chemists of terms used in biotechnology. *Pure Appl. Chem.* **1992**, *64*, 143–168.
69. Thévenot, D.R.; Toth, K.; Durst, R.A.; Wilson, G.S. Electrochemical biosensors: Recommended definitions and classification. *Biosens. Bioelectron.* **2001**, *16*, 121–131. [[CrossRef](#)]
70. Turner, A.P.F. Biosensors: Sense and sensibility. *Chem. Soc. Rev.* **2013**, *42*, 3184–3196. [[CrossRef](#)]
71. Bhalla, N.; Jolly, P.; Formisano, N.; Estrela, P. Introduction to biosensors. *Essays Biochem.* **2016**, *60*, 1–8. [[CrossRef](#)]

72. Singh, A.; Sharma, A.; Ahmed, A.; Sundramoorthy, A.; Furukawa, H.; Arya, S.; Khosla, A. Recent Advances in Electrochemical Biosensors: Applications, Challenges, and Future Scope. *Biosensors* **2021**, *11*, 336. [[CrossRef](#)]
73. Damborský, P.; Švitel, J.; Katrlík, J. Optical biosensors. *Essays Biochem.* **2016**, *60*, 91–100. [[CrossRef](#)] [[PubMed](#)]
74. Chen, C.; Wang, J. Optical biosensors: An exhaustive and comprehensive review. *Analyst* **2020**, *145*, 1605–1628. [[CrossRef](#)]
75. Grieshaber, D.; MacKenzie, R.; Vörös, J.; Reimhult, E. Electrochemical Biosensors—Sensor Principles and Architectures. *Sensors* **2008**, *8*, 1400–1458. [[CrossRef](#)] [[PubMed](#)]
76. Lazanas, A.C. Electrochemical Impedance Spectroscopy—A Tutorial. *ACS Meas. Sci. Au* **2023**, *3*, 162–193. [[CrossRef](#)] [[PubMed](#)]
77. Randviir, E.P.; Banks, C.E. A review of electrochemical impedance spectroscopy for bioanalytical sensors. *Anal. Methods* **2022**, *14*, 4602–4624. [[CrossRef](#)]
78. Venton, B.J.; DiScenza, D.J. *Voltammetry*; Elsevier: Amsterdam, The Netherlands, 2020. [[CrossRef](#)]
79. Elgrishi, N.; Rountree, K.J.; McCarthy, B.D.; Rountree, E.S.; Eisenhart, T.T.; Dempsey, J.L. A Practical Beginner's Guide to Cyclic Voltammetry. *J. Chem. Educ.* **2017**, *95*, 197–206. [[CrossRef](#)]
80. Lutz, R.; Bujard, H. Independent and tight regulation of transcriptional units in *Escherichia coli* via the LacR/O, the TetR/O and AraC/I1-I2 regulatory elements. *Nucleic Acids Res.* **1997**, *25*, 1203–1210. [[CrossRef](#)]
81. Liu, X.; Yang, H.; Xu, Z.; Liu, R.; Zuo, H.; Chen, Z.; Wang, X.; Xia, C.; Zhang, Y.; Ning, B.; et al. A novel biosensor based on antibody controlled isothermal strand displacement amplification (ACISDA) system. *Biosens. Bioelectron.* **2022**, *209*, 114185. [[CrossRef](#)]
82. Taylor, N.D.; Garruss, A.S.; Moretti, R.; Chan, S.; Arbing, M.A.; Gascio, D.; Rogers, J.K.; Isaacs, F.J.; Kosuri, S.; Baker, D.; et al. Engineering an allosteric transcription factor to respond to new ligands. *Nat. Methods* **2015**, *13*, 177–183. [[CrossRef](#)]
83. Oliveira, B.B.; Veigas, B.; Baptista, P.V. Isothermal Amplification of Nucleic Acids: The Race for the Next 'Gold Standard'. *Front. Sens.* **2021**, *2*, 752600. [[CrossRef](#)]
84. Du, Y.-C.; Jiang, H.-X.; Huo, Y.-F.; Han, G.-M.; Kong, D.-M. Optimization of strand displacement amplification-sensitized G-quadruplex DNAzyme-based sensing system and its application in activity detection of uracil-DNA glycosylase. *Biosens. Bioelectron.* **2016**, *77*, 971–977. [[CrossRef](#)]
85. Wang, W.; Peng, Y.; Wu, J.; Zhang, M.; Li, Q.; Zhao, Z.; Liu, M.; Wang, J.; Cao, G.; Bai, J.; et al. Ultrasensitive Detection of 17 $\beta$ -Estradiol (E2) Based on Multistep Isothermal Amplification. *Anal. Chem.* **2021**, *93*, 4488–4496. [[CrossRef](#)] [[PubMed](#)]
86. Verma, S.; Ghuge, S.A.; Ravichandiran, V.; Ranjan, N. Spectroscopic studies of Thioflavin-T binding to c-Myc G-quadruplex DNA. *Spectrochim. Acta Part A Mol. Biomol. Spectrosc.* **2018**, *212*, 388–395. [[CrossRef](#)] [[PubMed](#)]
87. Mohanty, J.; Barooah, N.; Dhamodharan, V.; Harikrishna, S.; Pradeepkumar, P.I.; Bhasikuttan, A.C. Thioflavin T as an Efficient Inducer and Selective Fluorescent Sensor for the Human Telomeric G-Quadruplex DNA. *J. Am. Chem. Soc.* **2012**, *135*, 367–376. [[CrossRef](#)] [[PubMed](#)]
88. Fan, L.; Peng, Y.; Ning, B.; Wei, H.; Gao, Z.; Bai, J.; Guo, L. A tri-functional probe mediated exponential amplification strategy for highly sensitive detection of Dnmt1 and UDG activities at single-cell level. *Anal. Chim. Acta* **2019**, *1103*, 164–173. [[CrossRef](#)]
89. Cheng, Y.; Wang, H.; Zhuo, Y.; Song, D.; Li, C.; Zhu, A.; Long, F. Reusable smartphone-facilitated mobile fluorescence biosensor for rapid and sensitive on-site quantitative detection of trace pollutants. *Biosens. Bioelectron.* **2021**, *199*, 113863. [[CrossRef](#)]
90. Chaudhary, N.; Yadav, A.K.; Sharma, J.G.; Solanki, P.R. Designing and characterization of a highly sensitive and selective biosensing platform for ciprofloxacin detection utilizing lanthanum oxide nanoparticles. *J. Environ. Chem. Eng.* **2021**, *9*, 106771. [[CrossRef](#)]
91. Escudero, A.; Beccero, A.; Carrillo-Carrion, C.; Nunez, N.; Zyuzin, M.; Laguna, M.; Gonzalez-Mancebo, D.; Ocana, M.; Parak, W. Rare earth based nanostructured materials: Synthesis, functionalization, properties and bioimaging and biosensing applications. *Nanophotonics* **2017**, *6*, 881–921. [[CrossRef](#)]
92. Sovizi, R.; Mirzakhani, S. A chemiresistor sensor modified with lanthanum oxide nanoparticles as a highly sensitive and selective sensor for dimethylamine at room temperature. *New J. Chem.* **2020**, *44*, 4927–4934. [[CrossRef](#)]
93. Zepf, V. An Overview of the Usefulness and Strategic Value of Rare Earth Metals. In *Rare Earths Industry: Technological, Economic, and Environmental Implications*; Elsevier Inc.: Amsterdam, The Netherlands, 2015; pp. 3–17. [[CrossRef](#)]
94. Yadav, A.K.; Dhiman, T.K.; Lakshmi, G.B.V.S.; Berlina, A.N.; Solanki, P.R. A highly sensitive label-free amperometric biosensor for norfloxacin detection based on chitosan-yttria nanocomposite. *Int. J. Biol. Macromol.* **2020**, *151*, 566–575. [[CrossRef](#)]
95. Ermolaeva, T.N.; Kalmykova, E.N. Piezoelectric immunosensors: Analytical potentials and outlooks. *Russ. Chem. Rev.* **2006**, *75*, 397–409. [[CrossRef](#)]
96. Vaughan, R.D.; Guibault, G.G. Piezoelectric Immunosensors. In *Piezoelectric Sensors*; Springer: Berlin/Heidelberg, Germany, 2006; pp. 237–280. [[CrossRef](#)]
97. Kim, S.N.; Rusling, J.F.; Papadimitrakopoulos, F. Carbon Nanotubes for Electronic and Electrochemical Detection of Biomolecules. *Adv. Mater.* **2007**, *19*, 3214–3228. [[CrossRef](#)]
98. Yang, W.; Thordarson, P.; Gooding, J.J.; Ringer, S.P.; Braet, F. Carbon nanotubes for biological and biomedical applications. *Nanotechnology* **2007**, *18*, 412001. [[CrossRef](#)]
99. Wang, J.; Lin, Y. Functionalized carbon nanotubes and nanofibers for biosensing applications. *TrAC Trends Anal. Chem.* **2008**, *27*, 619–626. [[CrossRef](#)]
100. Bizina, E.V.; Farafonova, O.V.; Zolotareva, N.I.; Grazhulene, S.S.; Ermolaeva, T.N. A Piezoelectric Immunosensor Based on Magnetic Carbon Nanocomposites for the Determination of Ciprofloxacin. *J. Anal. Chem.* **2022**, *77*, 458–465. [[CrossRef](#)]

101. Hu, G.; Sheng, W.; Zhang, Y.; Wu, X.; Wang, S. A novel and sensitive fluorescence immunoassay for the detection of fluoroquinolones in animal-derived foods using upconversion nanoparticles as labels. *Anal. Bioanal. Chem.* **2015**, *407*, 8487–8496. [[CrossRef](#)] [[PubMed](#)]
102. Shi, Q.; Huang, J.; Sun, Y.; Deng, R.; Teng, M.; Li, Q.; Yang, Y.; Hu, X.; Zhang, Z.; Zhang, G. A SERS-based multiple immunonanoprobe for ultrasensitive detection of neomycin and quinolone antibiotics via a lateral flow assay. *Microchim. Acta* **2018**, *185*, 84. [[CrossRef](#)]
103. Zhuo, Y.-X.; Xu, W.-J.; Yuan, C.; Song, D.; Xiang-Zhi, H.; Feng, L. Rapid detection of norfloxacin in water by evanescent wave fiber optic biosensor. *China Environ. Sci.* **2022**, *42*, 2283–2288.
104. Chen, Y.; Chen, Q.; Han, M.; Liu, J.; Zhao, P.; He, L.; Zhang, Y.; Niu, Y.; Yang, W.; Zhang, L. Near-infrared fluorescence-based multiplex lateral flow immunoassay for the simultaneous detection of four antibiotic residue families in milk. *Biosens. Bioelectron.* **2016**, *79*, 430–434. [[CrossRef](#)]
105. Sheng, W.; Li, S.; Liu, Y.; Wang, J.; Zhang, Y.; Wang, S. Visual and rapid lateral flow immunochromatographic assay for enrofloxacin using dyed polymer microspheres and quantum dots. *Microchim. Acta* **2017**, *184*, 4313–4321. [[CrossRef](#)]
106. Byzova, N.A.; Smirnova, N.; Zherdev, A.; Eremin, S.; Shanin, I.; Lei, H.; Sun, Y.; Dzantiev, B. Rapid immunochromatographic assay for ofloxacin in animal original foodstuffs using native antisera labeled by colloidal gold. *Talanta* **2014**, *119*, 125–132. [[CrossRef](#)]
107. Taranova, N.A.; Berlina, A.N.; Zherdev, A.V.; Dzantiev, B.B. ‘Traffic light’ immunochromatographic test based on multicolor quantum dots for the simultaneous detection of several antibiotics in milk. *Biosens. Bioelectron.* **2015**, *63*, 255–261. [[CrossRef](#)] [[PubMed](#)]
108. El Kojok, H.; El Darra, N.; Khalli, M.; Capovilla, A.; Pennaccio, A.; Staiano, M.; Camarca, A.; D’Auria, S.; Varriale, A. Fluorescence polarization assay to detect the presence of traces of ciprofloxacin. *Sci. Rep.* **2020**, *10*, 4550. [[CrossRef](#)]
109. Zhang, Z.; Zhang, M.; Wu, X.; Chang, Z.; Lee, Y.; Huy, B.; Sakthivel, K.; Liu, J.; Jiang, G. Upconversion fluorescence resonance energy transfer—A novel approach for sensitive detection of fluoroquinolones in water samples. *Microchem. J.* **2015**, *124*, 181–187. [[CrossRef](#)]
110. Lamarca, R.S.; de Faria, R.A.D.; Zanoni, M.V.B.; Nalin, M.; de Lima Gomes, P.C.F.; Messaddeq, Y. Simple, fast and environmentally friendly method to determine ciprofloxacin in wastewater samples based on an impedimetric immunosensor. *RSC Adv.* **2020**, *10*, 1838–1847. [[CrossRef](#)]
111. Giroud, F.; Gorgy, K.; Gondran, C.; Cosnier, S.; Pinacho, D.; Marco, M.-P.; Sánchez-Baeza, F. Impedimetric Immunosensor Based on a Polypyrrole—Antibiotic Model Film for the Label-Free Picomolar Detection of Ciprofloxacin. *Anal. Chem.* **2009**, *81*, 8405–8409. [[CrossRef](#)] [[PubMed](#)]
112. Ionescu, R.E.; Jaffrezic-Renault, N.; Bouffier, L.; Gondran, C.; Cosnier, S.; Pinacho, D.; Marco, M.-P.; Sánchez-Baeza, F.; Healy, T.; Martelet, C. Impedimetric immunosensor for the specific label free detection of ciprofloxacin antibiotic. *Biosens. Bioelectron.* **2007**, *23*, 549–555. [[CrossRef](#)] [[PubMed](#)]
113. Pinacho, D.G.; Sánchez-Baeza, F.; Pividori, M.-I.; Marco, M.-P. Electrochemical detection of fluoroquinolone antibiotics in milk using a magneto immunosensor. *Sensors* **2014**, *14*, 15965–15980. [[CrossRef](#)] [[PubMed](#)]
114. Tsekenis, G.; Garifallou, G.; Davis, F.; Millner, P.; Pinacho, D.; Sánchez-Baeza, F.; Marco, M.-P.; Gibson, T.; Higson, S. Detection of Fluoroquinolone Antibiotics in Milk via a Labelless Immunoassay Based upon an Alternating Current Impedance Protocol. *Anal. Chem.* **2008**, *80*, 9233–9239. [[CrossRef](#)]
115. Liu, B.; Li, M.; Zhao, Y.; Pan, M.; Gu, Y.; Sheng, W.; Fang, G.; Wang, S. A Sensitive Electrochemical Immunosensor Based on PAMAM Dendrimer-Encapsulated Au for Detection of Norfloxacin in Animal-Derived Foods. *Sensors* **2018**, *18*, 1946. [[CrossRef](#)]
116. Zang, S.; Liu, Y.; Lin, M.; Kang, J.; Sun, Y.; Lei, H. A dual amplified electrochemical immunosensor for ofloxacin: Polypyrrole film-Au nanocluster as the matrix and multi-enzyme-antibody functionalized gold nanorod as the label. *Electrochim. Acta* **2013**, *90*, 246–253. [[CrossRef](#)]
117. He, Z.; Zang, S.; Liu, Y.; He, Y.; Lei, H. A multi-walled carbon nanotubes-poly(L-lysine) modified enantioselective immunosensor for ofloxacin by using multi-enzyme-labeled gold nanoflower as signal enhancer. *Biosens. Bioelectron.* **2015**, *73*, 85–92. [[CrossRef](#)]
118. Kim, B.; Lim, D.; Jin, H.; Lee, H.; Namgung, S.; Ko, Y.; Park, S.; Hong, S. Family-selective detection of antibiotics using antibody-functionalized carbon nanotube sensors. *Sens. Actuators B Chem.* **2012**, *166–167*, 193–199. [[CrossRef](#)]
119. Adachi, T.; Nakamura, Y. Aptamers: A Review of Their Chemical Properties and Modifications for Therapeutic Application. *Molecules* **2019**, *24*, 4229. [[CrossRef](#)] [[PubMed](#)]
120. Zhou, J.; Rossi, J. Aptamers as targeted therapeutics: Current potential and challenges. *Nat. Rev. Drug Discov.* **2017**, *16*, 181–202. [[CrossRef](#)]
121. Arshavsky-Graham, S.; Heuer, C.; Jiang, X.; Segal, E. Aptasensors versus immunosensors—Which will prevail? *Eng. Life Sci.* **2022**, *22*, 319–333. [[CrossRef](#)]
122. Xu, Y.; Jiang, X.; Zhou, Y.; Ma, M.; Wang, M.; Ying, B. Systematic Evolution of Ligands by Exponential Enrichment Technologies and Aptamer-Based Applications: Recent Progress and Challenges in Precision Medicine of Infectious Diseases. *Front. Biotechnol. Biotechnol.* **2021**, *9*, 704077. [[CrossRef](#)]
123. Tuerk, C.; Gold, L. Systematic Evolution of Ligands by Exponential Enrichment: RNA Ligands to Bacteriophage T4 DNA Polymerase. *Science* **1990**, *249*, 505–510. [[CrossRef](#)]

124. Yan, Z.; Wang, L.; Zhou, X.; Yan, R.; Zhang, D.; Wang, S.; Su, L.; Zhou, S. Fluorescent aptasensor for ofloxacin detection based on the aggregation of gold nanoparticles and its effect on quenching the fluorescence of Rhodamine, B. *Spectrochim. Acta Part A Mol. Biomol. Spectrosc.* **2019**, *221*, 117203. [[CrossRef](#)]
125. Hammami, I.; Alabdallah, N.M.; Al Jomaa, A.; Kamoun, M. Gold nanoparticles: Synthesis properties and applications. *J. King Saud Univ. Sci.* **2021**, *33*, 101560. [[CrossRef](#)]
126. Zhan, S.; Wu, Y.; He, L.; Wang, F.; Zhan, X.; Zhou, P.; Qiu, S. A silver-specific DNA-based bio-assay for Ag(i) detection via the aggregation of unmodified gold nanoparticles in aqueous solution coupled with resonance Rayleigh scattering. *Anal. Methods* **2012**, *4*, 3997. [[CrossRef](#)]
127. Beija, M.; Afonso, C.A.M.; Martinho, J.M.G. Synthesis and applications of Rhodamine derivatives as fluorescent probes. *Chem. Soc. Rev.* **2009**, *38*, 2410. [[CrossRef](#)]
128. Heidarian, S.M.T.; Sani, A.T.; Danesh, N.M.; Ramezani, M.; Alibolandi, M.; Gerayelou, G.; Abnous, K.; Taghdisi, S.M. A novel electrochemical approach for the ultrasensitive detection of fluoroquinolones based on a double-labelled aptamer to surpass complementary strands of aptamer lying flat. *Sens. Actuators B Chem.* **2021**, *334*, 129632. [[CrossRef](#)]
129. Mahmoudpour, M.; Kholafazad-kordasht, H.; Dolatabadi, J.E.N.; Hasanzadeh, M.; Rad, A.H.; Torbati, M. Sensitive aptasensing of ciprofloxacin residues in raw milk samples using reduced graphene oxide and nanogold-functionalized poly(amidoamine) dendrimer: An innovative apta-platform towards electroanalysis of antibiotics. *Anal. Chim. Acta* **2021**, *1174*, 338736. [[CrossRef](#)]
130. Javed, R.; Zia, M.; Naz, S.; Aisida, S.O.; Ain, N.U.; Ao, Q. Role of capping agents in the application of nanoparticles in biomedicine and environmental remediation: Recent trends and future prospects. *J. Nanobiotechnol.* **2020**, *18*, 172. [[CrossRef](#)]
131. Niu, Z.; Li, Y. Removal and Utilization of Capping Agents in Nanocatalysis. *Chem. Mater.* **2013**, *26*, 72–83. [[CrossRef](#)]
132. Abbasi, E.; Aval, S.; Akbarzadeh, A.; Milani, M.; Nasrabadi, H.; Joo, S.; Hanifehpour, Y.; Nejati-Koshki, K.; Pashaei-Asl, R. Dendrimers: Synthesis, applications, and properties. *Nanoscale Res. Lett.* **2014**, *9*, 247. [[CrossRef](#)]
133. Wang, M.; Hu, M.; Liu, J.; Guo, C.; Peng, D.; Jia, Q.; He, L.; Zhang, Z.; Du, M. Covalent organic framework-based electrochemical aptasensors for the ultrasensitive detection of antibiotics. *Biosens. Bioelectron.* **2019**, *132*, 8–16. [[CrossRef](#)]
134. Zhang, Z.; Liu, Q.; Zhang, M.; You, F.; Hao, N.; Ding, C.; Wang, K. Simultaneous detection of enrofloxacin and ciprofloxacin in milk using a bias potentials controlling-based photoelectrochemical aptasensor. *J. Hazard. Mater.* **2021**, *416*, 125988. [[CrossRef](#)]
135. Zhang, Z.; Zhang, M.; Xu, Y.; Wen, Z.; Ding, C.; Guo, Y.; Hao, N.; Wang, K. Bi<sup>3+</sup> engineered black anatase titania coupled with graphene for effective tobramycin photoelectrochemical detection. *Sens. Actuators B Chem.* **2020**, *321*, 128464. [[CrossRef](#)]
136. Liu, X.; Su, L.; Zhu, L.; Gao, X.; Wang, Y.; Bai, F.; Tang, Y.; Li, J. Hybrid material for enrofloxacin sensing based on aptamer-functionalized magnetic nanoparticle conjugated with upconversion nanopropes. *Sens. Actuators B Chem.* **2016**, *233*, 394–401. [[CrossRef](#)]
137. Dolati, S.; Ramezani, M.; Nabavinia, M.S.; Soheili, V.; Abnous, K.; Taghdisi, S.M. Selection of specific aptamer against enrofloxacin and fabrication of graphene oxide based label-free fluorescent assay. *Anal. Biochem.* **2018**, *549*, 124–129. [[CrossRef](#)] [[PubMed](#)]
138. Liu, X.; Ren, J.; Su, L.; Gao, X.; Tang, Y.; Ma, T.; Zhu, L.; Li, J. Novel hybrid probe based on double recognition of aptamer-molecularly imprinted polymer grafted on upconversion nanoparticles for enrofloxacin sensing. *Biosens. Bioelectron.* **2017**, *87*, 203–208. [[CrossRef](#)] [[PubMed](#)]
139. Zhou, X.; Wang, L.; Shen, G.; Zhang, D.; Xie, J.; Mamut, A.; Huang, W.; Zhou, S. Colorimetric determination of ofloxacin using unmodified aptamers and the aggregation of gold nanoparticles. *Microchim. Acta* **2018**, *185*, 355. [[CrossRef](#)]
140. Lavaee, P.; Danesh, N.M.; Ramezani, M.; Abnous, K.; Taghdisi, S.M. Colorimetric aptamer based assay for the determination of fluoroquinolones by triggering the reduction-catalyzing activity of gold nanoparticles. *Microchim. Acta* **2017**, *184*, 2039–2045. [[CrossRef](#)]
141. Hu, X.; Goud, K.; Kumar, V.; Catanante, G.; Li, Z.; Zhu, Z.; Marty, J. Disposable electrochemical aptasensor based on carbon nanotubes- V2O5-chitosan nanocomposite for detection of ciprofloxacin. *Sens. Actuators B Chem.* **2018**, *268*, 278–286. [[CrossRef](#)]
142. Abnous, K.; Danesh, N.M.; Alibolandi, M.; Ramezani, M.; Taghdisi, S.M.; Emrani, A.S. A novel electrochemical aptasensor for ultrasensitive detection of fluoroquinolones based on single-stranded DNA-binding protein. *Sens. Actuators B Chem.* **2017**, *240*, 100–106. [[CrossRef](#)]
143. Cheraghi, S.; Taher, M.A.; Karimi-Maleh, H.; Faghih-Mirzaei, E. A nanostructure label-free DNA biosensor for ciprofloxacin analysis as a chemotherapeutic agent: An experimental and theoretical investigation. *New J. Chem.* **2017**, *41*, 4985–4989. [[CrossRef](#)]
144. Diab, N.; Abu-Shqair, I.; Salim, R.; Al-Subu, M. The Behavior of Ciprofloxacin at a DNA Modified Glassy Carbon Electrodes. *Int. J. Electrochem. Sci.* **2014**, *9*, 1771–1783. [[CrossRef](#)]
145. Pilehvar, S.; Reinemann, C.; Bottari, F.; Vanderleyden, E.; Van Vlierberghe, S.; Blust, R.; Strehlitz, B.; De Wael, K. A joint action of aptamers and gold nanoparticles chemically trapped on a glassy carbon support for the electrochemical sensing of ofloxacin. *Sens. Actuators B Chem.* **2017**, *240*, 1024–1035. [[CrossRef](#)]
146. Bekir, K.; Beltifa, A.; Maatouk, F.; Khedary, N.H.; Barhoumi, H.; Mansour, H.B. DNA as a Next-Generation Biomonitoring Tool of Hospital Effluent Contamination. *Sustainability* **2022**, *14*, 2440. [[CrossRef](#)]
147. You, F.; Wen, Z.; Yuan, R.; Ding, L.; Wei, J.; Qian, J.; Long, L.; Wang, K. Selective and ultrasensitive detection of ciprofloxacin in milk using a photoelectrochemical aptasensor based on Ti<sub>3</sub>C<sub>2</sub>/Bi<sub>4</sub>VO<sub>8</sub>Br/TiO<sub>2</sub> nanocomposite. *J. Electroanal. Chem.* **2022**, *914*, 116285. [[CrossRef](#)]
148. Nguyen, H.H.; Lee, S.H.; Lee, U.J.; Fermin, C.D.; Kim, M. Immobilized Enzymes in Biosensor Applications. *Materials* **2019**, *12*, 121. [[CrossRef](#)] [[PubMed](#)]

149. Rebollar-Pérez, G.; Campos-Terán, J.; Ornelas-Soto, N.; Méndez-Albores, A.; Torres, E. Biosensors based on oxidative enzymes for detection of environmental pollutants. *Biocatalysis* **2016**, *1*, 118–129. [[CrossRef](#)]
150. Bertolino, F.A.; De Vito, I.E.; Messina, G.A.; Fernández, H.; Raba, J. Microfluidic-enzymatic biosensor with immobilized tyrosinase for electrochemical detection of pipemidic acid in pharmaceutical samples. *J. Electroanal. Chem.* **2011**, *651*, 204–210. [[CrossRef](#)]
151. Esen, E.; Yazgan, İ.; Demirkol, D.O. Biezymatic fluorecence detection based on paraoxonase and laccase on anthracene-sequestered polyamic acid films: A novel approach for inhibition-based sensors. *Mater. Today Commun.* **2020**, *25*, 101672. [[CrossRef](#)]
152. Furlong, C.E.; Marsillach, J.; Jarvik, G.P.; Costa, L.G. Paraoxonases-1, -2 and -3: What are their functions? *Chem. Interact.* **2016**, *259*, 51–62. [[CrossRef](#)] [[PubMed](#)]
153. Torriero, A.A.J.; Salinas, E.; Raba, J.; Silber, J.J. Sensitive determination of ciprofloxacin and norfloxacin in biological fluids using an enzymatic rotating biosensor. *Biosens. Bioelectron.* **2006**, *22*, 109–115. [[CrossRef](#)]
154. Cardoso, A.R.; Carneiro, L.P.T.; Cabral-Miranda, G.; Bachmann, M.F.; Sales, M.G.F. Employing bacteria machinery for antibiotic detection: Using DNA gyrase for ciprofloxacin detection. *Chem. Eng. J.* **2020**, *409*, 128135. [[CrossRef](#)]
155. Yan, Y.; Zhou, F.; Wang, Q.; Huang, Y. A sensitive electrochemical biosensor for quinolones detection based on Cu<sup>2+</sup>-modulated signal amplification. *Microchem. J.* **2023**, *190*, 108636. [[CrossRef](#)]
156. Uivarosi, V. Metal complexes of quinolone antibiotics and their applications: An update. *Molecules* **2013**, *18*, 11153–11197. [[CrossRef](#)]
157. Arshavsky-Graham, S.; Urmann, K.; Salama, R.; Massad-Ivanir, N.; Walter, J.; Scheper, T.; Segal, E. Aptamers vs. antibodies as capture probes in optical porous silicon biosensors. *Analyst* **2020**, *145*, 4991–5003. [[CrossRef](#)]
158. Thurner, F.; Alatraktchi, F.A.A. Recent advances in electrochemical biosensing of aflatoxin M1 in milk—A mini review. *Microchem. J.* **2023**, *190*, 108594. [[CrossRef](#)]
159. Peng, Z.; Xie, X.; Tan, Q.; Kang, H.; Cui, J.; Zhang, X.; Li, W.; Feng, G. Blood glucose sensors and recent advances: A review. *J. Innov. Opt. Heal. Sci.* **2022**, *15*, 2230003. [[CrossRef](#)]
160. Zhang, J.; Wang, Y.; Xu, X.; Yang, X. Specifically colorimetric recognition of calcium, strontium, and barium ions using 2-mercaptosuccinic acid-functionalized gold nanoparticles and its use in reliable detection of calcium ion in water. *Analyst* **2011**, *136*, 3865–3868. [[CrossRef](#)] [[PubMed](#)]
161. Bozzano, L. *Handbook of Milk Composition*; Academic Press: Cambridge, MA, USA, 1995.
162. Parthasarathy, R.; Monette, C.E.; Bracero, S.; Saha, M.S. Methods for field measurement of antibiotic concentrations: Limitations and outlook. *FEMS Microbiol. Ecol.* **2018**, *94*, 105. [[CrossRef](#)]
163. Campisi, S.; Schiavoni, M.; Chan-Thaw, C.; Villa, A. Untangling the Role of the Capping Agent in Nanocatalysis: Recent Advances and Perspectives. *Catalysts* **2016**, *6*, 185. [[CrossRef](#)]
164. Mao, Y.; Dang, M.; Zhang, J.; Huang, X.; Qiao, M.; Song, L.; Zhao, Q.; Ding, M.; Wang, Y.; Li, Z.; et al. Peptide amphiphile inspired self-assembled, ordered gold nanocomposites for improved sensitivity of electrochemical immunosensor: Applications in determining the total aflatoxin amount in food stuffs. *Talanta* **2022**, *247*, 123532. [[CrossRef](#)] [[PubMed](#)]
165. Singh, J.; Dutta, T.; Kim, K.-H.; Rawat, M.; Samddar, P.; Kumar, P. 'Green' synthesis of metals and their oxide nanoparticles: Applications for environmental remediation. *J. Nanobiotechnol.* **2018**, *16*, 84. [[CrossRef](#)]
166. Makarov, V.V.; Love, A.; Sinitsyna, O.; Makarova, S.; Yaminsky, I.; Taliansky, M.; Kalinina, N. 'Green' Nanotechnologies: Synthesis of Metal Nanoparticles Using Plants. *Acta Naturae* **2014**, *6*, 35–44. [[CrossRef](#)]

**Disclaimer/Publisher's Note:** The statements, opinions and data contained in all publications are solely those of the individual author(s) and contributor(s) and not of MDPI and/or the editor(s). MDPI and/or the editor(s) disclaim responsibility for any injury to people or property resulting from any ideas, methods, instructions or products referred to in the content.